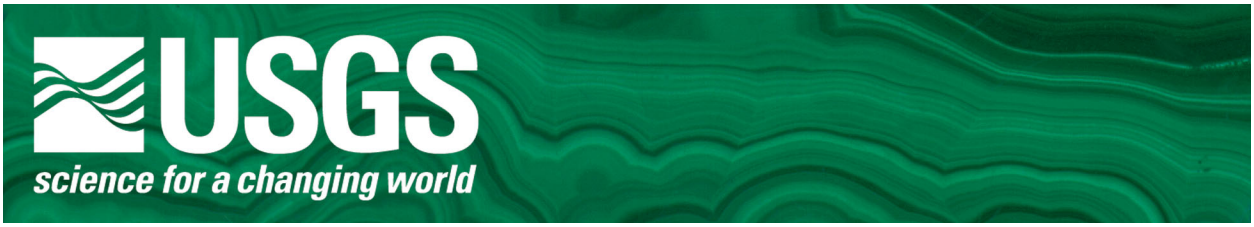

CHAPTER 2

Comparison of Carlin-type Au Deposits in the United States, China, and Indonesia: Implications for Genetic Models and Exploration

By Albert H. Hofstra[1], and Odin D. Christensen[2]

Open-File Report: 02–131

2002

U.S. DEPARTMENT OF THE INTERIOR
U.S. GEOLOGICAL SURVEY

[1]U.S. Geological Survey, Mail Stop 973, Box 25046,
Denver Federal Center, Denver, Colorado 80225
[2]Newmont Mining Corporation, 10101 East Dry Creek Road, Englewood, CO 80112

Table of Contents

INTRODUCTION

DEPOSIT CHARACTERISTICS
- Orebody shape and control
- Mineralogical characteristics
- Geochemical Characteristics

TECTONICS

GUIZHOU AREA

QINLING AREA

MESEL Au DEPOSIT

SOURCE of WATER, CO_2, and H_2S

SUMMARY and CONCLUSIONS

REFERENCES

List of Figures

Figure 2-1. Location of Carlin-type Au deposits worldwide in Nevada in P.R. China. The Chinese deposits are present in the Qinling (fold belt) and Guizhou (Dian-Qian-Gui) areas.
Figure 2-2. Pie charts of amounts of Au in Carlin-type deposits in the U.S. (Nevada), China, and Indonesia. Nevada contains the largest amount of reserves and resources
Figure 2-3. Characteristics of Carlin-type deposits.
Figure 2-4. Schematic model for northern Carlin trend Au deposits.
Figure 2-5. Other sedimentary rock-hosted Au deposit in Nevada.
Figure 2-6. Crustal structures associated with Carlin-type deposits in the Carlin trend area, northern Nevada.
Figure 2-7. Mine-scale alteration zoning of Carlin-type deposits illustrated from the Carlin trend, Nevada.
Figure 2-8 Mine-scale alteration zoning at the Mesel Au deposit, Indonesia. Modified from Garwin (1994).
Figure 2-9. Gold-bearing arsenian pyrite rim on diagenetic pyrite from Post/Betze.
Figure 2-10. Reflected light view of dark arsenian pyrite that locally rims bright diagenetic pyrite from Mesel, Indonesia.
Figure 2-11. Photograph of orpiment-realgar vein at the Getchell Mine, Getchell trend, northern Nevada.

Figure 2-12. Photograph of crystalline specimens of late ore stage orpiment and realgar from the Guizhou area, China.
Figure 2-13. Photograph of specimen of late ore stage stibnite from the Guizhou area, China.
Figure 2-14. Photographs of hand specimens of typical samples of late ore stage orpiment, stibnite, and calcite from Mesel, Indonesia.
Figure 2-15. Geochemical data from 27 different Carlin-type deposits in Nevada.
Figure 2-16. Geochemical data from 5 deposits in the Guizhou area relative to geochemical data from deposits in Nevada.
Figure 2-17. Geochemical data from 2 deposits in the Qinling area; the Laerma and Qiongmo Au deposits relative to geochemical.
Figure 2-18. Geochemical data from the Mesel Au deposit, Indonesia in relation to geochemical data from Nevada.
Figure 2-19. Photographs buffalo, northern Nevada and China.
Figure 2-20. Late Paleozoic and Mesozoic fold and thrust belts and Mesozoic Magmatism in the northern Great Basin.
Figure 2-21. Schematic east-west cross section of northern Nevada and northwestern Utah.
Figure 2-22. Sectional model for environment of Carlin-type Au deposits in northern Nevada.
Figure 2-23. Tectonic setting of northern Nevada in Lower Eocene time.
Figure 2-24. Tectonic setting of Carlin-type Au deposits in China.
Figure 2-25. Graph showing that the bulk of Au in both areas in China is in Triassic sedimentary rocks.
Figure 2-26. Geology and sedimentary rock-hosted Au deposits in the Guizhou (Dian-Qian-Gui) area.
Figure 2-27. Mineralization styles in the Guizhou area for Carlin-type deposits.
Figure 2-28. Generalized geologic features of the West Qinling area, China.
Figure 2-29. Schematic cross section through the Qinling orogenic belt, looking west.
Figure 2-30. Geology and cross section of the Dongbeizhai Au deposit, Qinling area, China.
Figure 2-31. Geologic setting of the Mesel Au deposit, Ratatotok District, Sulawesi, Indonesia.
Figure 3-32. Stratigraphic section at the Mesel Au deposit, Indonesia, showing location of Au ore in the Ratatotok limestone.
Figure 2-33. δD vs. $\delta^{18}O$ plot from Carlin-type Au deposits in northern Nevada.
Figure 2-34. Stable isotopic data from deposits in the Guizhou and Qinling areas
Figure 2-35. Plots of $\delta^{13}C$ vs. $\delta^{18}O$ data from altered rocks of late calcite veins from deposits in the Carlin trend, Jerritt Canyon, Cortez, and Alligator Ridge districts, northern Nevada.
Figure 2-36. $\delta^{13}C$ vs. $\delta^{18}O$ plots of data from the Mesel Au deposit, Indonesia (top panel) and Qinling and Guizhou areas, China (bottom panel).
Figure 2-37. Plots of $\delta^{34}S$ data from sedimentary rock-hosted and Carlin-type Au deposits in northern Nevada.
Figure 2-38. Plots of $\delta^{34}S$ data from sedimentary rock-hosted and Carlin-type Au deposits in Qinling and Guizhou areas in China and the Mesel Au deposit in Indonesia.
Figure 2-39. Summary of characteristics and features of Carlin-type Au deposits in China, Mesel Au deposit, Indonesia and Nevada.
Figure 2-40. Diverse origins of Carlin-type deposits in terms of fluid sources.
Figure 2-41. Frontiers in Exploration for Carlin-type Au deposits.

CHAPTER 2

Comparison of Carlin-type Au Deposits in the United States, China, and Indonesia: Implications for genetic models and exploration

By

Albert H. Hofstra, and Odin D. Christensen

INTRODUCTION

This chapter is a slightly modified version of an invited oral slide presentation that was presented on November 12, 2000 at the Society of Economic Geologists symposium "Janus II: Mineral Exploration for the 21st Century" at the Geological Society of America Annual Meeting in Reno, Nevada (Hofstra and Christensen, 2000). In addition to our own observations and data, the principal references used to produce parts of this chapter include: Hofstra and Cline (2000) for the deposits in the United States; Li, Z.P. and Peters (1998), Liu, J. and others (2000, 2001), Hu, R.Z. and others (2001), and Mao, J. and others (2001) for the deposits in China; and Turner and others (1994) and Garwin and others (1995) for the deposits in Indonesia. We want to thank our colleagues for insightful discussions, John Gray (Newmont) for providing samples from Mesel, and Bill Christiansen and Cindy Kester (USGS) for prompt isotopic analyses. A place name in this chapter differs from that used in the other chapters of this Open-File Report. Herein, we refer to the Dian-Qian-Gui area in China as the Guizhou area.

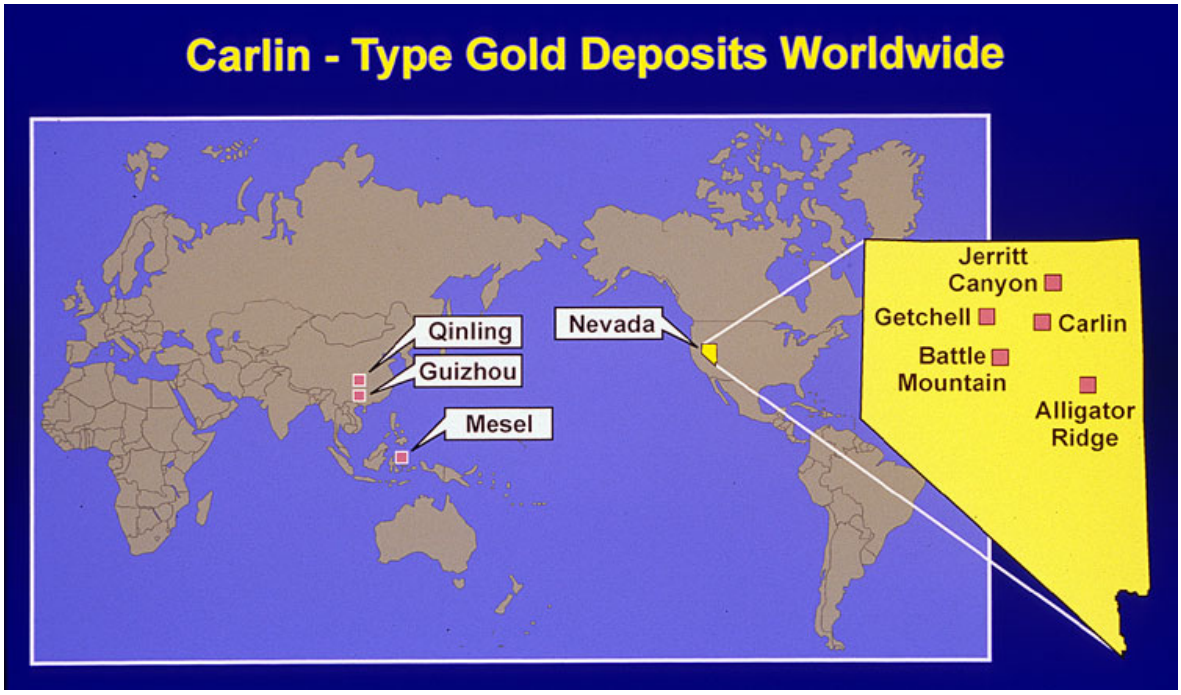

Figure 2-1. Location of Carlin-type Gold deposits worldwide in Nevada in P.R. China. The Chinese deposits are present in the Qinling (fold belt) and Guizhou (Dian-Qian-Gui) areas.

Sedimentary-rock-hosted disseminated Au deposits are often called Carlin-type regardless of their origins and are known in several places around the world. The purpose of this report is to determine whether deposits called Carlin-type in different parts of the world have similar or different origins. We chose to evaluate those in Nevada, the Guizhou and Qinling areas of China, and the Mesel Au deposit in Indonesia (fig. 2-1) because they have comparable data sets and we are more familiar with them. Since the deposits in each of the four selected areas have very similar characteristics, our main emphasis in this chapter is to compare their tectonic settings and stable isotopic data because this information places important constraints on genetic models. The amount of information available for the different areas is quite variable and there is much left to be resolved. Thus, this should be considered a progress report.

How significant are the Au deposits in each of these areas? Figure 2-2 shows that the U.S. deposits, mainly in Nevada, contain (production+reserves) more than 5000 t Au, those in China 450 t Au, and the Mesel Au deposit in Indonesia 65 t Au. The amount of Au in the Chinese deposits is similar to that estimated for those in Nevada in 1980. So it will be interesting see how these numbers change over the next 20 years. Although the amount of Au in the Mesel Au deposit is small, we thought it would be important to compare it to the others because it is in an island-arc setting and samples were available from the deposit for this study. The pie charts on figure 2-2 show that the Guizhou area contains more Au than the Qinling area and that the Carlin trend (CT) contains most of the Au in Nevada.

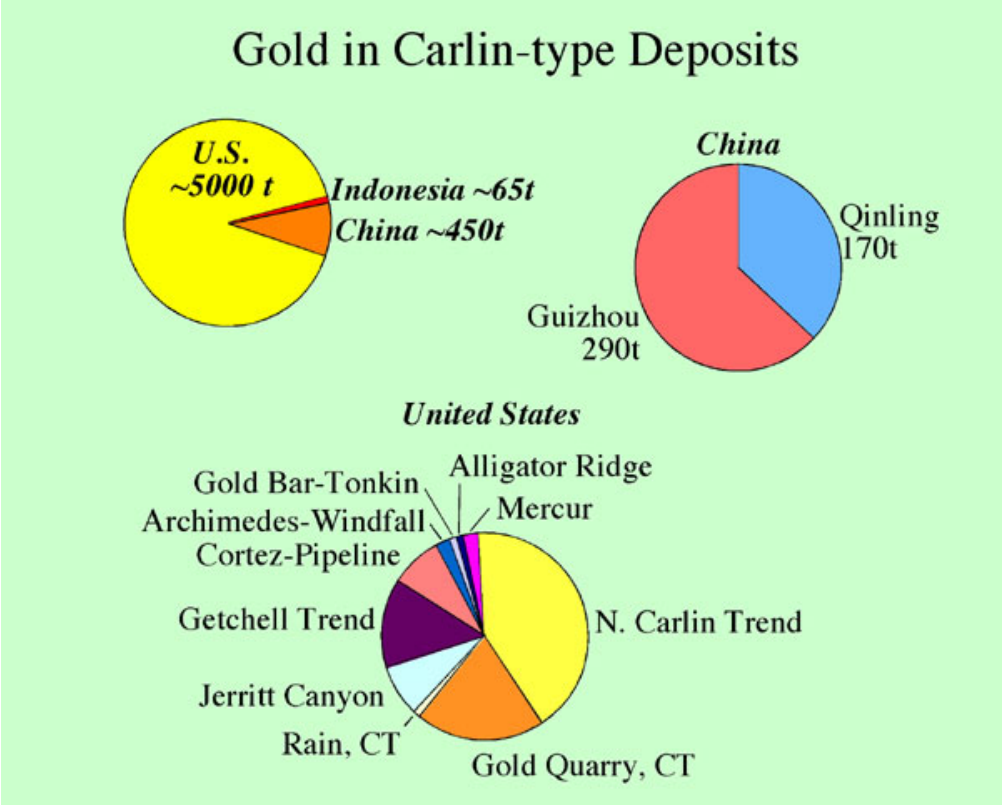

Figure 2-2. Pie charts of amounts of Au in Carlin-type deposits in the U.S. (Nevada), China, and Indonesia. Nevada contains the largest amount of reserves and resources.

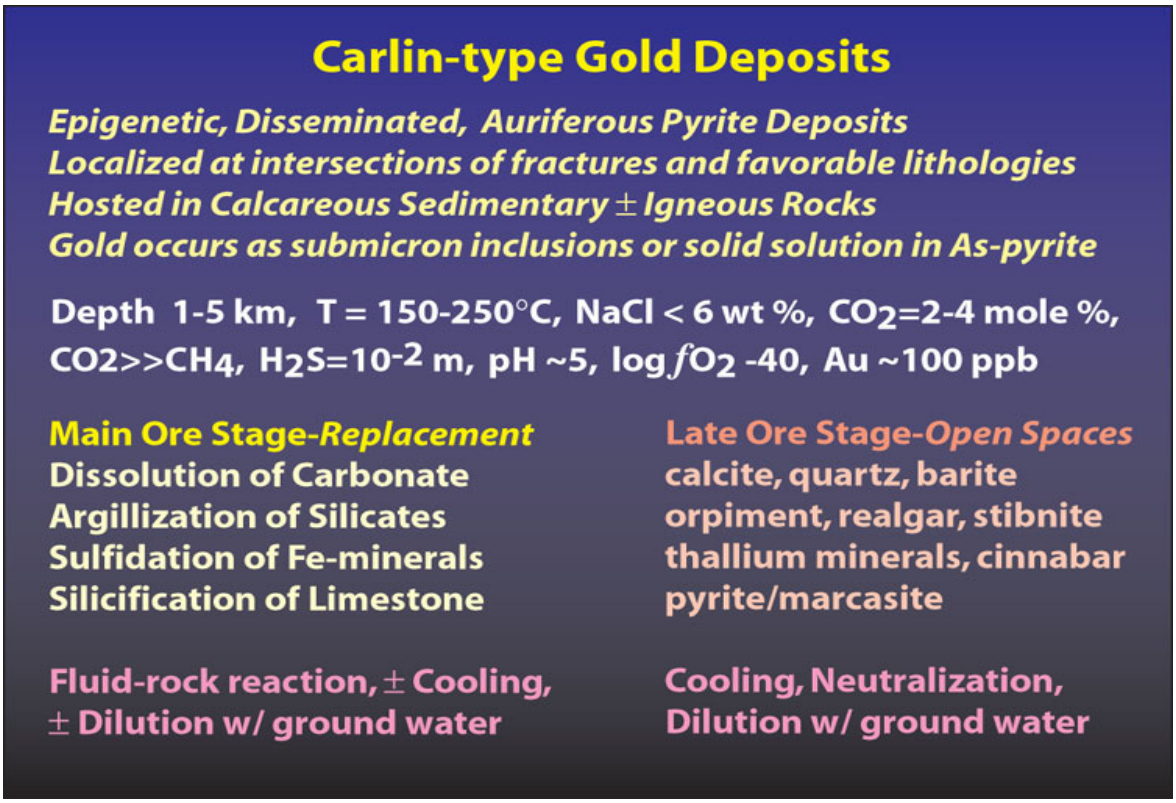

Figure 2-3. Characteristics of Carlin-type Au deposits.

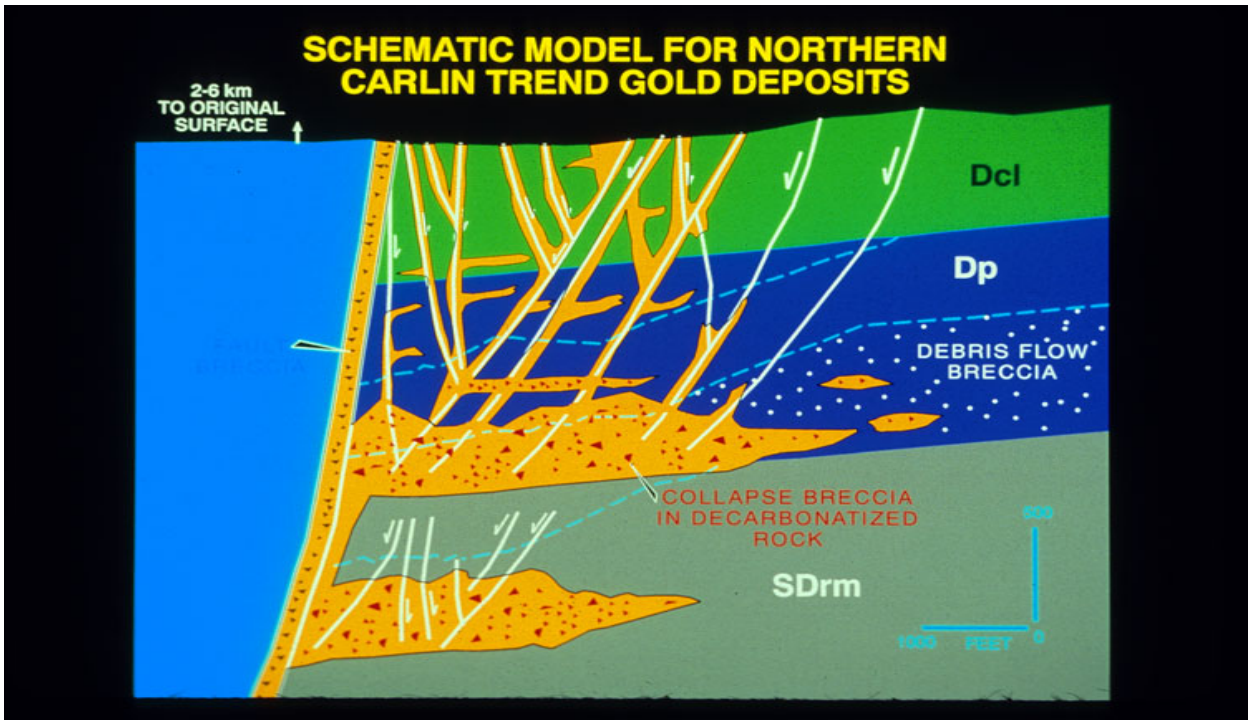

Figure 2-4. Schematic model for northern Carlin trend Au deposits. The deposits are both stratabound and localized along faults and others structures.

What is a Carlin-type deposit? Those in Nevada (fig. 2-3) are epigenetic disseminated auriferous pyrite deposits that are typically hosted in calcareous sedimentary rocks. Gold is present as submicron inclusions or solid solution in As-rich pyrite. The Au deposits formed where ore fluids moved up crustal structures, met less permeable cap rocks, and moved laterally into more permeable and reactive carbonate rocks. The relative importance of structural and stratigraphic controls on ore vary considerably from deposit to deposit (e.g. fig. 2-4 with ore in orange). The roots of the ore fluid systems are difficult to trace and somewhat cryptic, suggesting that we have more to learn about their hydrology. Their common alteration, mineralogy, and geochemical signatures are a direct expression of the physical and chemical environment in which they formed. General absence of boiling and presence of mineralized rock over vertical intervals of up to 1 km argues against a shallow depth of mineralization. Geologic reconstructions and fluid-inclusion data suggest that most Carlin-type Au deposits formed at depths of 2 to 5 km and at temperatures of about 200 ˚C. They formed from low salinity, CO_2 and H_2S-rich fluids that were moderately acidic and reduced. These fluids dissolved carbonate minerals, argillized silicate minerals , and sulfidized Fe-bearing minerals in the host rocks. Where there was sufficient cooling, the rocks also were silicified. Gold, As and other sulfide-complexed trace elements precipitated in pyrite as H_2S was consumed by reaction with Fe-bearing minerals. As a consequence, Fe generally is not introduced. Late ore stage quartz, calcite, barite, orpiment, realgar, and stibnite precipitated in open fractures and pores as the systems cooled and ore fluids mixed with local ground water.

Figure 2-5. Other sedimentary rock-hosted Au deposit in Nevada. These include sedex (stratiform-syngenetic), pluton-related (distal-disseminated Ag–Au), and epithermal (low-sulfidation/adularia-sericite Au) deposits.

Why is there so much confusion as to what a Carlin-type deposit is? There are four main reasons: (1) they are present in regions that also contain sedex, pluton-related, and epithermal sedimentary rock-hosted Au deposits(e.g. fig. 2-5); (2) Carlin-type Au deposits yield conflicting indications as to the source of ore fluids (see below); (3) in several districts, they lie in or adjacent to long-lived, deep-penetrating crustal structures that localized ore deposits of different types and ages (fig. 2-6). In the Carlin trend, Nevada each of these events deposited some Au, and in places, different types of Au mineralization are superimposed. This association is probably telling us something very important about their genesis; and (4) primary relationships are obscured by supergene weathering and oxidation. Unfortunately, most early studies did not recognize this complexity, which resulted in spurious interpretations as to the age and genesis of the deposits.

DEPOSIT CHARACTERISTICS

Carlin-type deposits in Nevada, China, and Indonesia have remarkably similar styles of alteration, Au-bearing arsenian pyrite, late ore-stage minerals, and geochemical signatures. The following figures show some of these characteristics.

Orebody shape and control

Figure 2-7 is a cross-section showing alteration at the Carlin Au deposit on the Carlin trend, Nevada and figure 2-8 is a cross section for the Mesel Au deposit, Indonesia. In both districts, alteration progresses outward from an absence of carbonate, through a dolomite stable zone, into calcareous rocks. Proximal kaolinite alterationprogresses outward into illite-stable alteration zones. The centers of the deposits are silicified. Fine-grained, arsenian pyrite is most abundant in proximal zones and diminishes outward.

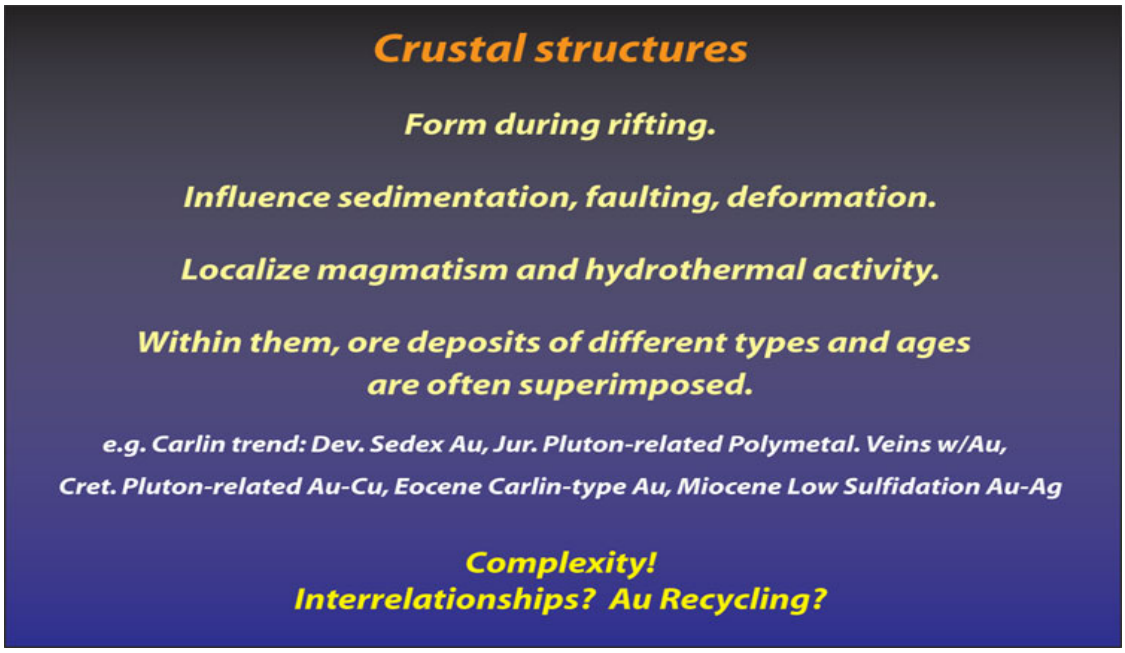

Figure 2-6. Crustal structures associated with Carlin-type deposits in the Carlin trend area, northern Nevada.

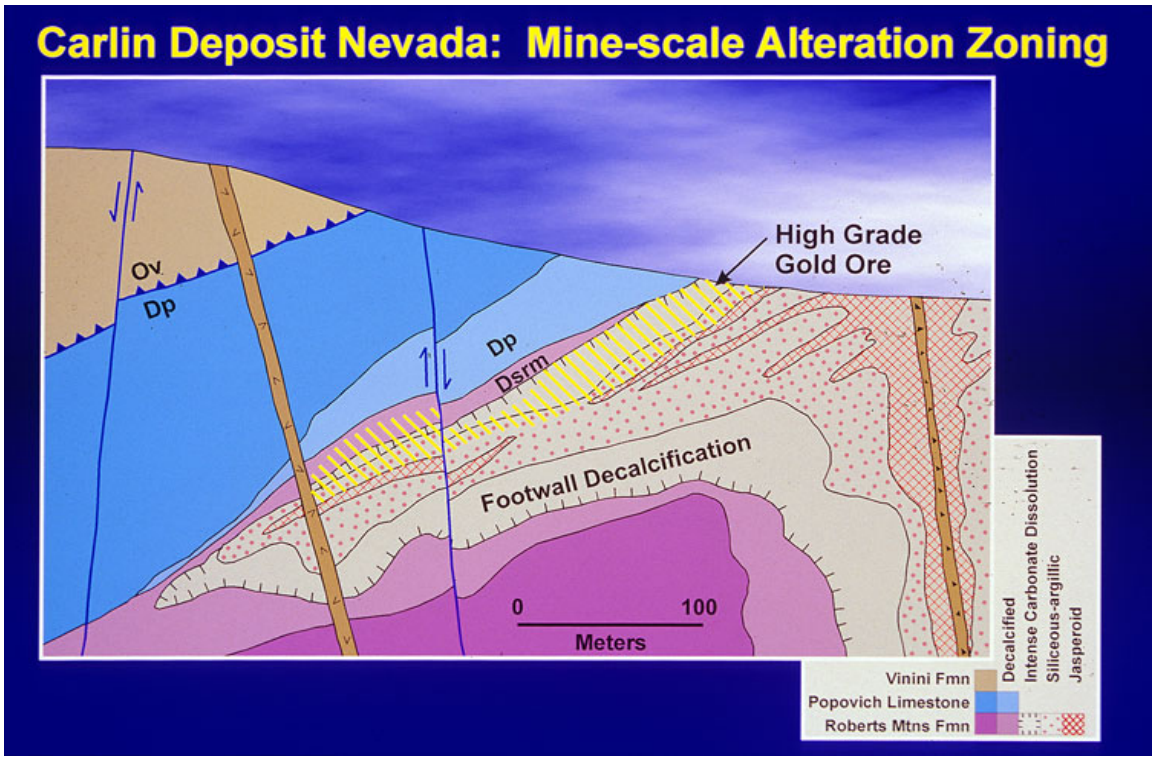

Figure 2-7. Mine-scale alteration zoning of Carlin-type deposits illustrated from the Carlin Au deposit Carlin trend, Nevada.

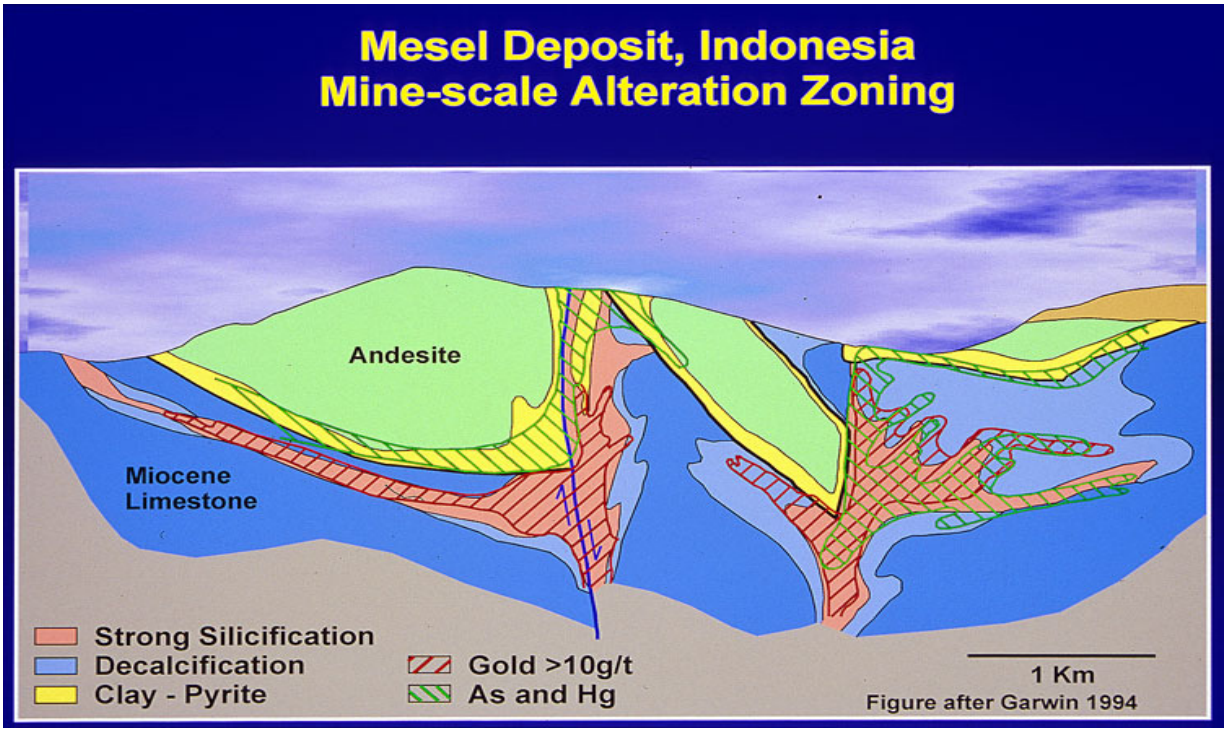

Figure 2-8. Mine-scale alteration zoning at the Mesel Au deposit, Indonesia. Modified from Garwin (1994).

Mineralogical characteristics

Figure 2-9 shows a classic Au-bearing arsenian pyrite rim on diagenetic pyrite from Post/Betze (SIMS maps for As and Au on the left and reflected light view on the right). Figure 2-10 is a reflected light view of dark arsenian pyrite that locally rims bright diagenetic pyrite from Mesel Au deposit, Indonesia. The arsenian pyrite at Mesel contains up to 1 % Au. Figure 2-11 shows an orpiment-realgar vein at the Getchell Au deposit, northern Nevada. Figure 2-12 shows some nice specimens of late ore-stage orpiment and realgar from the Guizhou area in China. Figure 2-13 is a specimen of late ore stage stibnite from the Guizhou area, China. Figure 2-14 shows more typical samples of late ore stage orpiment, stibnite, and calcite from the Mesel Au deposit, Indonesia.

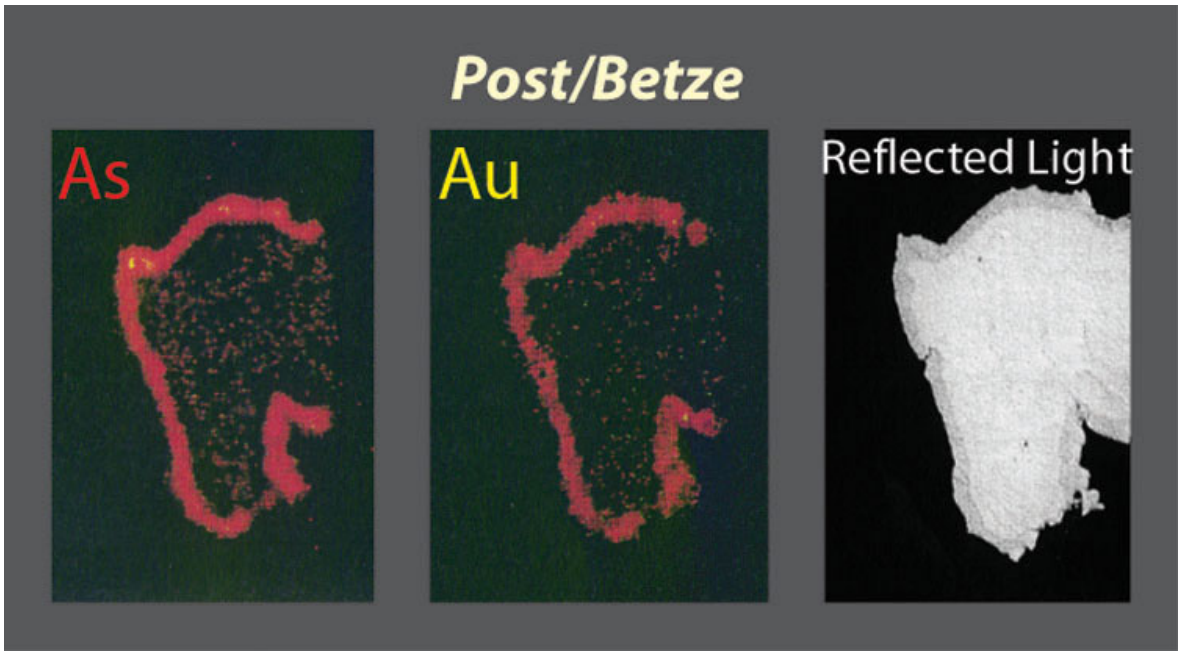

Figure 2-9. Gold-bearing arsenian pyrite rim on diagenetic pyrite from Post/Betze (SIMS maps for As and Au on the left and reflected light view on the right).

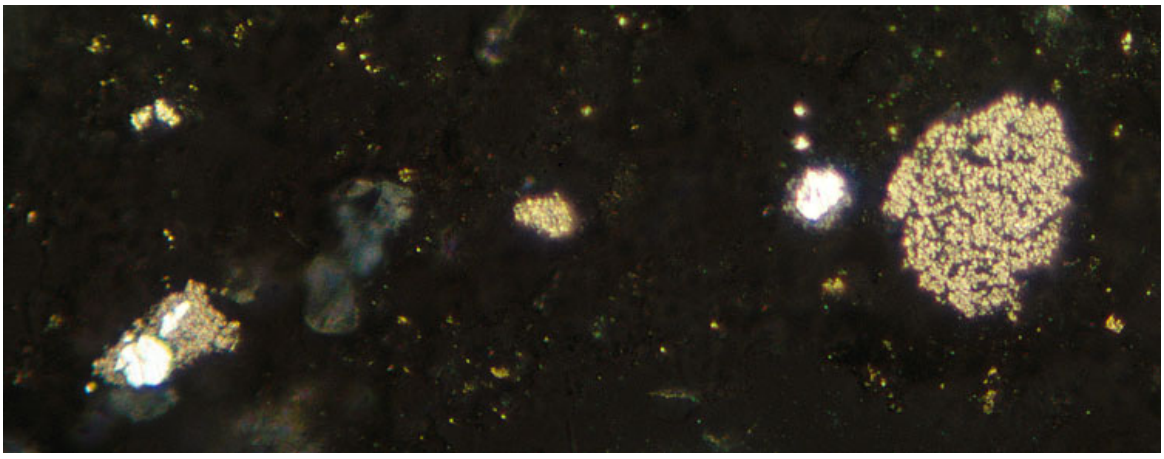

Figure 2-10. Reflected light view of dark arsenian pyrite that locally rims bright diagenetic pyrite from Mesel.

Figure 2-11. Orpiment-realgar vein at the Getchell Mine, Getchell trend, northern Nevada.

Figure 2-12. Crystalline specimens of late ore stage orpiment and realgar from the Guizhou area, China.

Figure 2-13. Specimen of late ore stage stibnite from the Guizhou area, China.

Figure 2-14. Photographs of hand specimens of typical samples of late ore stage orpiment, stibnite, and calcite from Mesel, Indonesia.

Geochemical Characteristics

The next few figures show that element enrichments in the deposits also are very similar. Enrichment factors were calculated by dividing the average element concentrations of the ores by the average element concentrations of the crust. On these plots, the elements are arranged from the classic Carlin-type suite on the left, through Ag and base metals to Mo and W on the right. Figure 2-15 shows data from 27 different Carlin-type deposits in Nevada. Figure 2-16 shows data from 5 deposits in the Guizhou area relative to the data from deposits in Nevada (in black).

We only have data from 2 deposits in the Qinling area; the Laerma and Qiongmo Au deposits (fig. 2-17). They have higher Cu and Mo concentrations, but geochemically are otherwise similar to those in Nevada. Element enrichments at the Mesel Au deposit (fig. 2-18) are no different from the deposits in Nevada. The remarkable similarities among these deposits essentially require that they formed from fluids with very similar chemical compositions; namely, low to moderate salinity, H_2S-rich fluids.

The critical questions, then, are: did all of these deposits form in the same type of hydrothermal system with ore fluids derived from similar sources in analogous geologic settings (e.g. pair of buffalo; fig. 2-19A), or were they from fluids derived from different sources in distinct settings (convergent evolution e.g. yak; fig. 2-19B)? To address these questions, we compared the tectonic settings and stable isotopic data for deposits in each area.

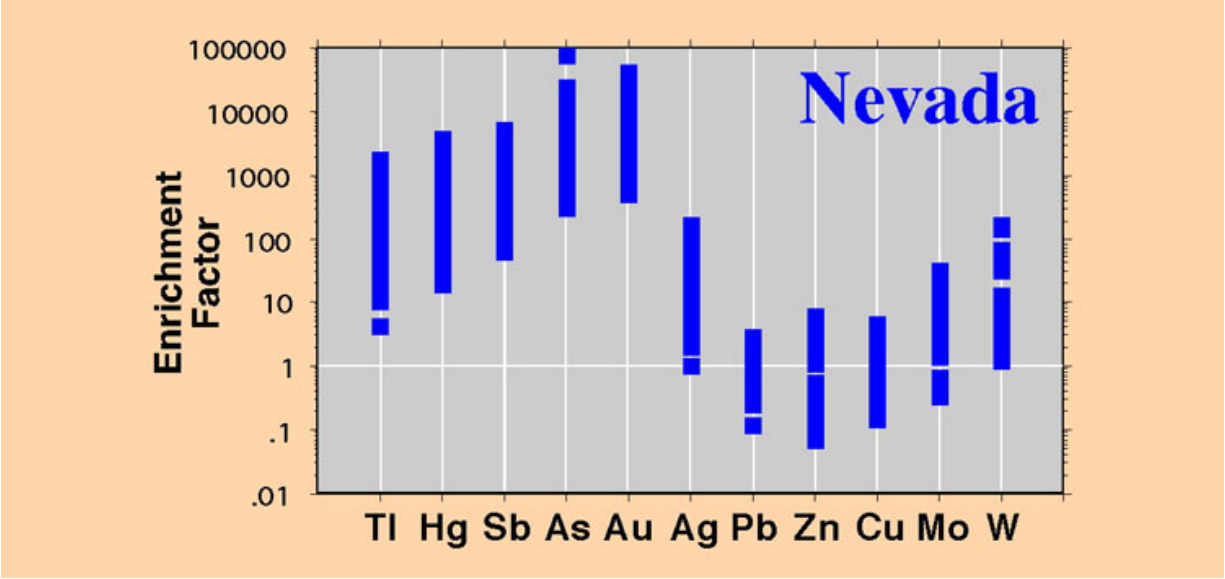

Figure 2-15. Geochemical data from 27 different Carlin-type deposits in Nevada.

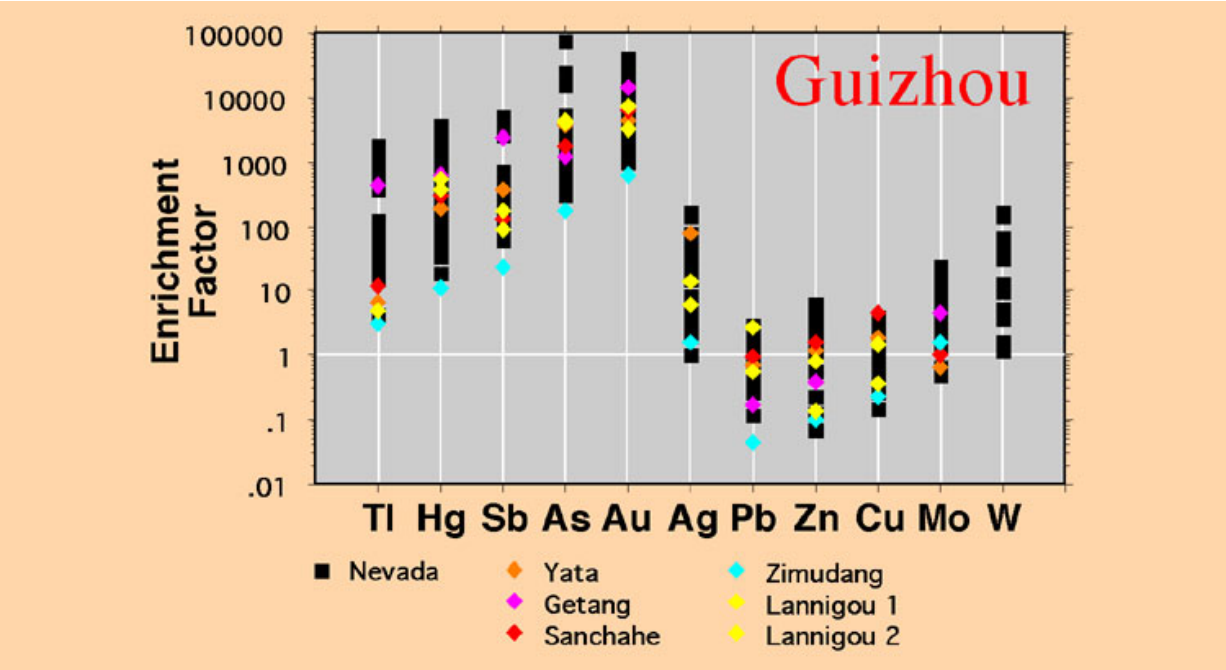

Figure 2-16. Geochemical data from 5 deposits in the Guizhou area relative to geochemical data from deposits in Nevada (in black).

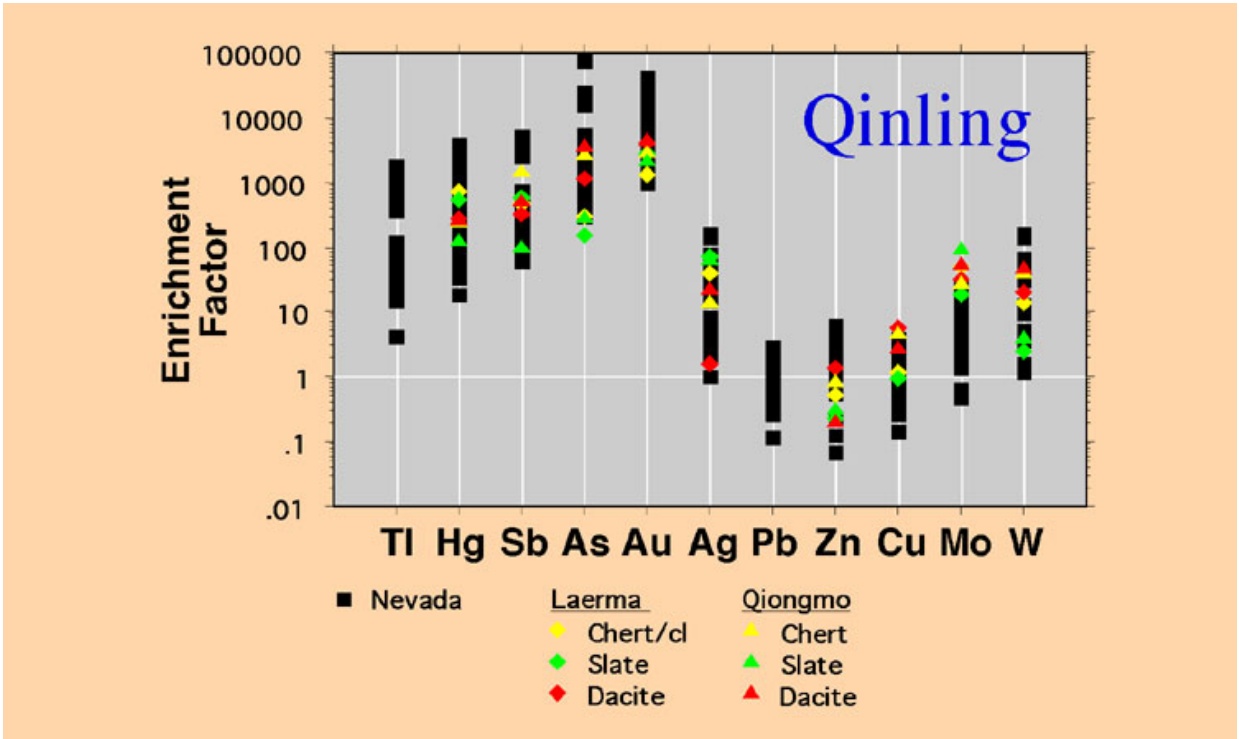

Figure 2-17. Geochemical data from 2 deposits in the Qinling area; the Laerma and Qiongmo deposits relative to geochemical Data in Nevada (in black).

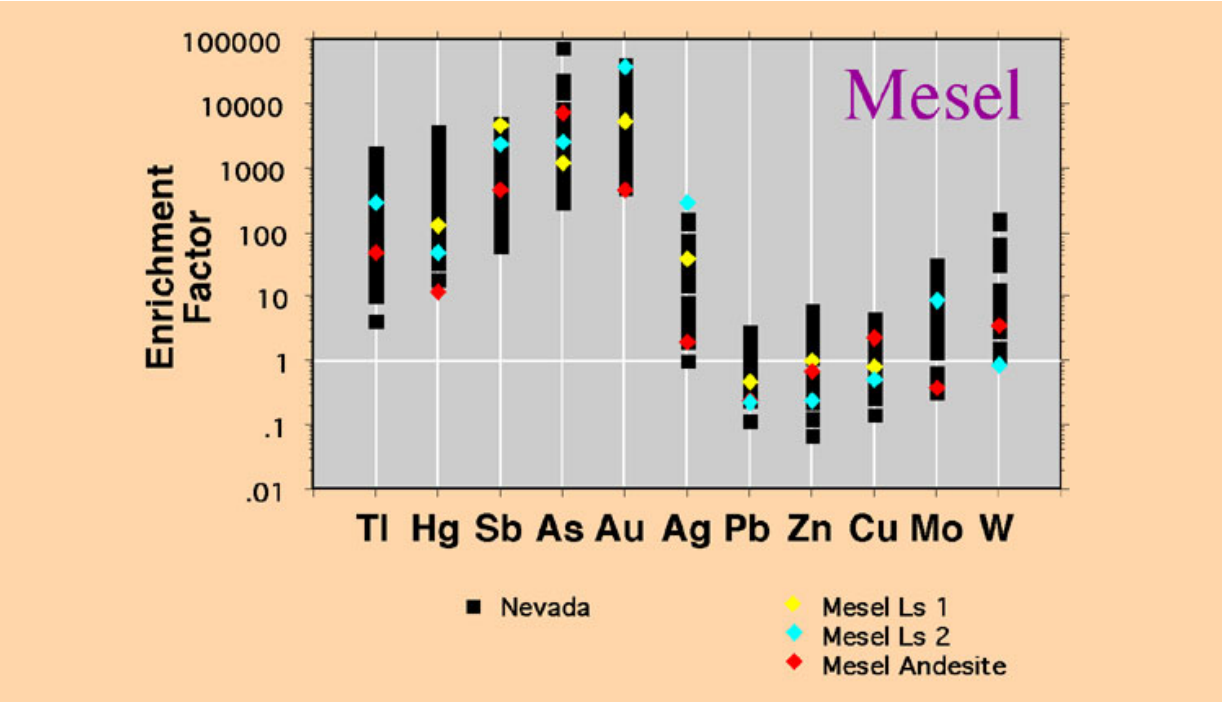

Figure 2-18. Geochemical data from the Mesel deposit, Indonesia in relation to geochemical data from Nevada (in black).

Figure 2-19. Photographs of buffalo. (*A-top*) American buffalo, northern Nevada. (B-bottom) Water buffalo, Guizhou area, China.

TECTONIC SETTING

Carlin-type deposits in the northern Great Basin are restricted to a small part of the North American Cordillera (black dots on fig. 2-20), and formed over a short period of time in the Late Eocene. They are located in an over-thickened late Proterozoic through Devonian miogeocline that was deformed by successive Late Paleozoic and Mesozoic orogenies that included intrusion of Jurassic and Cretaceous plutons (pink areas on fig. 2-20). Figure 2-21 is a schematic cross-section showing the relation of gold deposits to crustal faults, stratigraphic sequences (J-T=Jurassic-Tertiary, M-P Missippian-Permian, and C-D= Cambrian Devonian), allochthons, crystalline basement, and the Sr_i .706 line. It shows that most of the Carlin-type Au deposits (yellow ovals) are hosted in lower Paleozoic miogeoclinal carbonate rocks of diverse facies that are either structurally overlain by siliciclastic rocks of the Roberts Mountains allochthon, or are stratigraphically overlain by siliciclastic rocks deposited in the resulting foredeep. As mentioned earlier, the major Carlin-type Au districts are located along deep-crustal faults produced by Proterozoic rifting that localized successive igneous and hydrothermal events. The vast majority of the Au is in Devonian rocks, a feature that is a consequence of the physical and chemical properties of these lithologies, and their position below less permeable cap rocks.

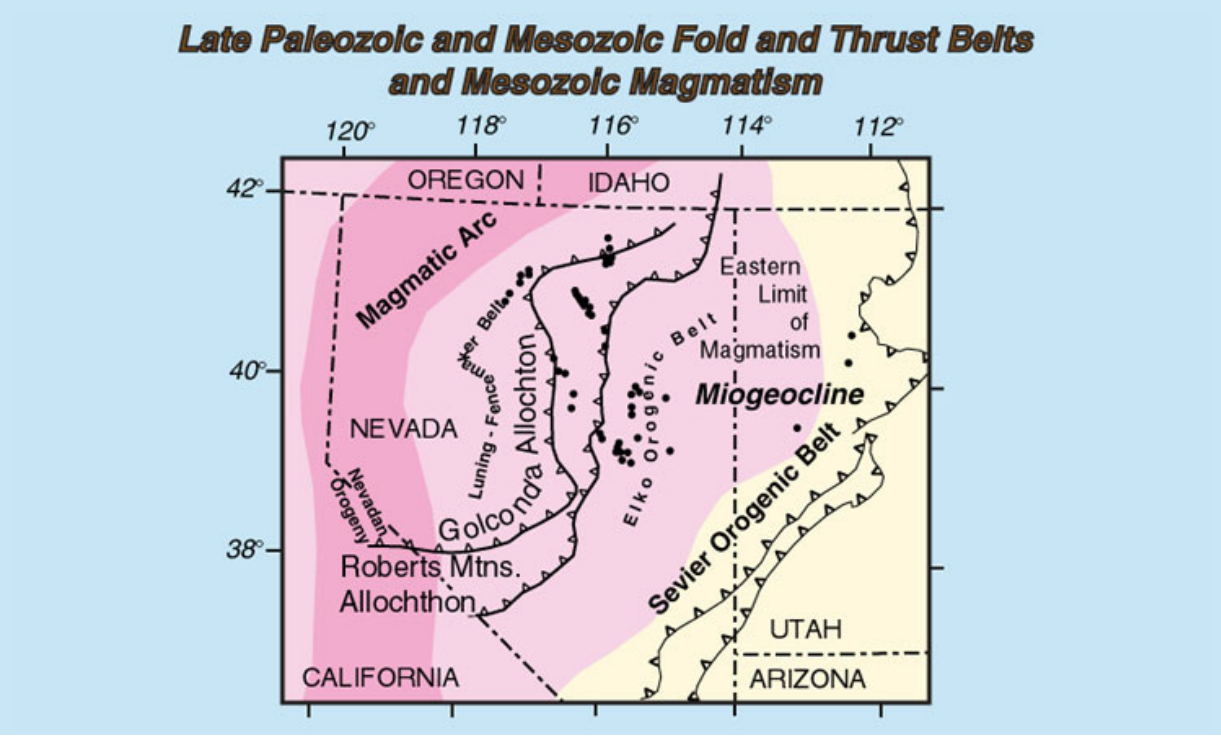

Figure 2-20. Late Paleozoic and Mesozoic fold and thrust belts and Mesozoic Magmatism in the northern Great Basin.

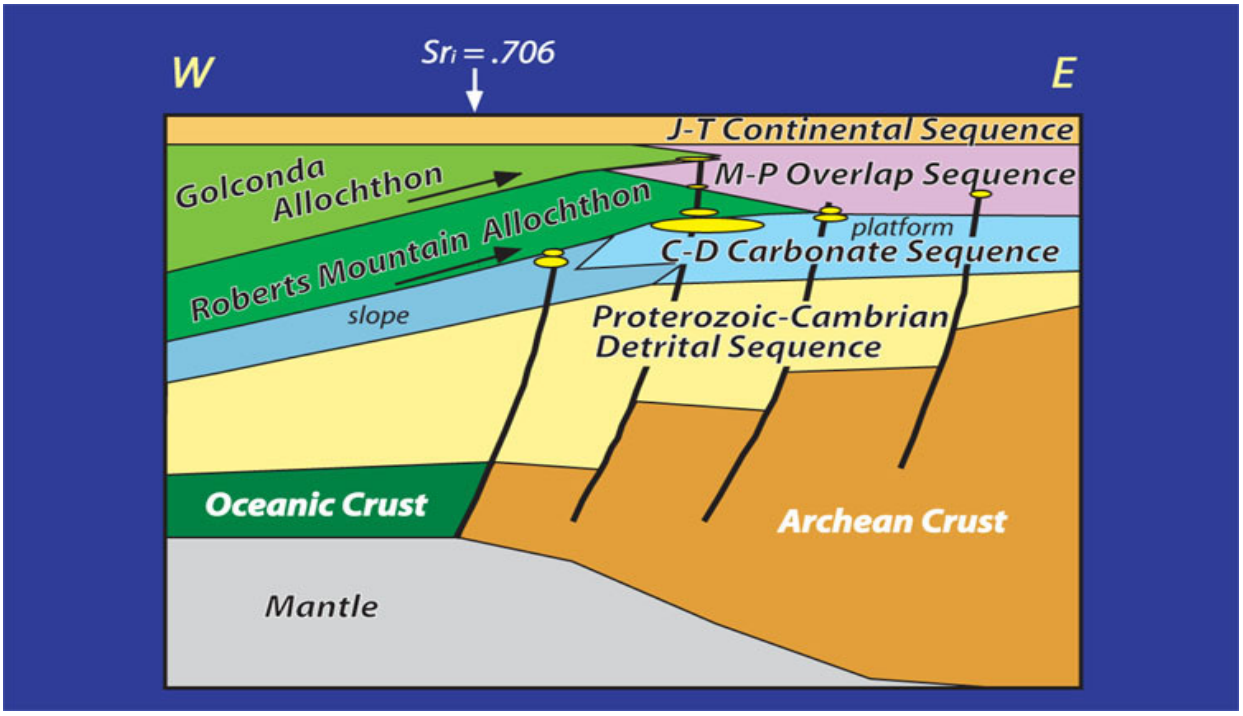

Figure 2-21. Schematic east-west cross section of northern Nevada and northwestern Utah, showing Achaean crust, oceanic crust, overlying stratigraphic and tectonic sequences, fault zones, and location of sedimentary rock-hosted Au-Ag deposits (adapted from Hofstra and Cline, 2000).

The Carlin-type Au deposits formed after a period of flat subduction in Late Cretaceous and Early Tertiary time, which produced a magmatic gap in the arc and resulted in cooling of the crust. They formed in the Late Eocene, as the Farallon plate fell away from the base of the crust and sank into the mantle (slab roll back on fig. 2-22). At this time, the Yellowstone mantle plume is inferred by some workers to have been located below the subduction zone. The Farallon plate warped along an east-west axis producing a diffuse east-west-trending, south-migrating, subduction-related magmatic belt that contains a number of porphyry systems (orange area on fig. 2-23). Carlin-type Au deposits (black dots on fig. 2-23) are restricted to this belt and are contemporaneous with magmatism, but do not show consistant spatial relations to major magmatic centers within it. Rather, they are localized along crustal structures. The deposits formed at, or soon after, the onset of extension in this belt (green arrows on fig. 2-23), but before, or lateral to, areas of large magnitude extension (core complexes on fig. 2-23). Transtension along crustal structures produced dilatant zones that focused flow of hydrothermal fluids and localized the deposits. The setting permits that fluids ascending along these conduits could have been magmatic, meteoric, or metamorphic in origin. Mixing between deep and shallow fluids was probably inevitable

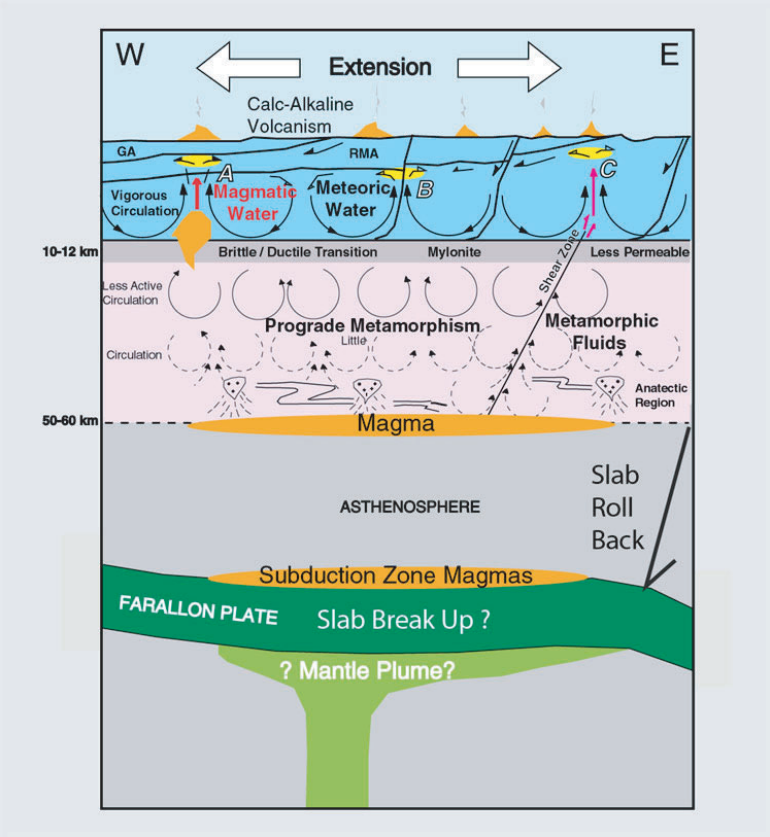

Fig. 2-22. Sectional model of Carlin-type Au deposits in northern Nevada.

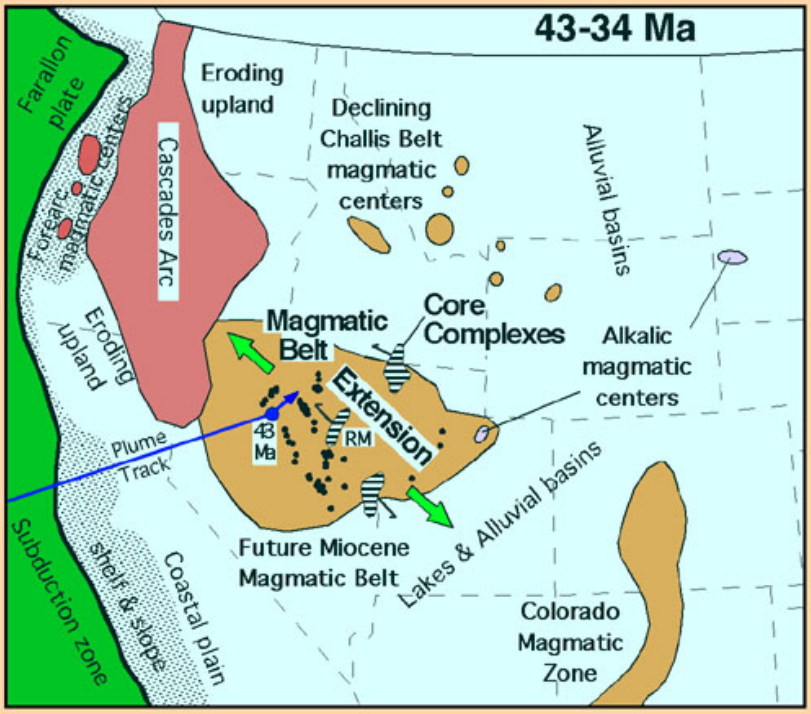

Figure 2-23. Tectonic setting of northern Nevada in Lower Eocene time.

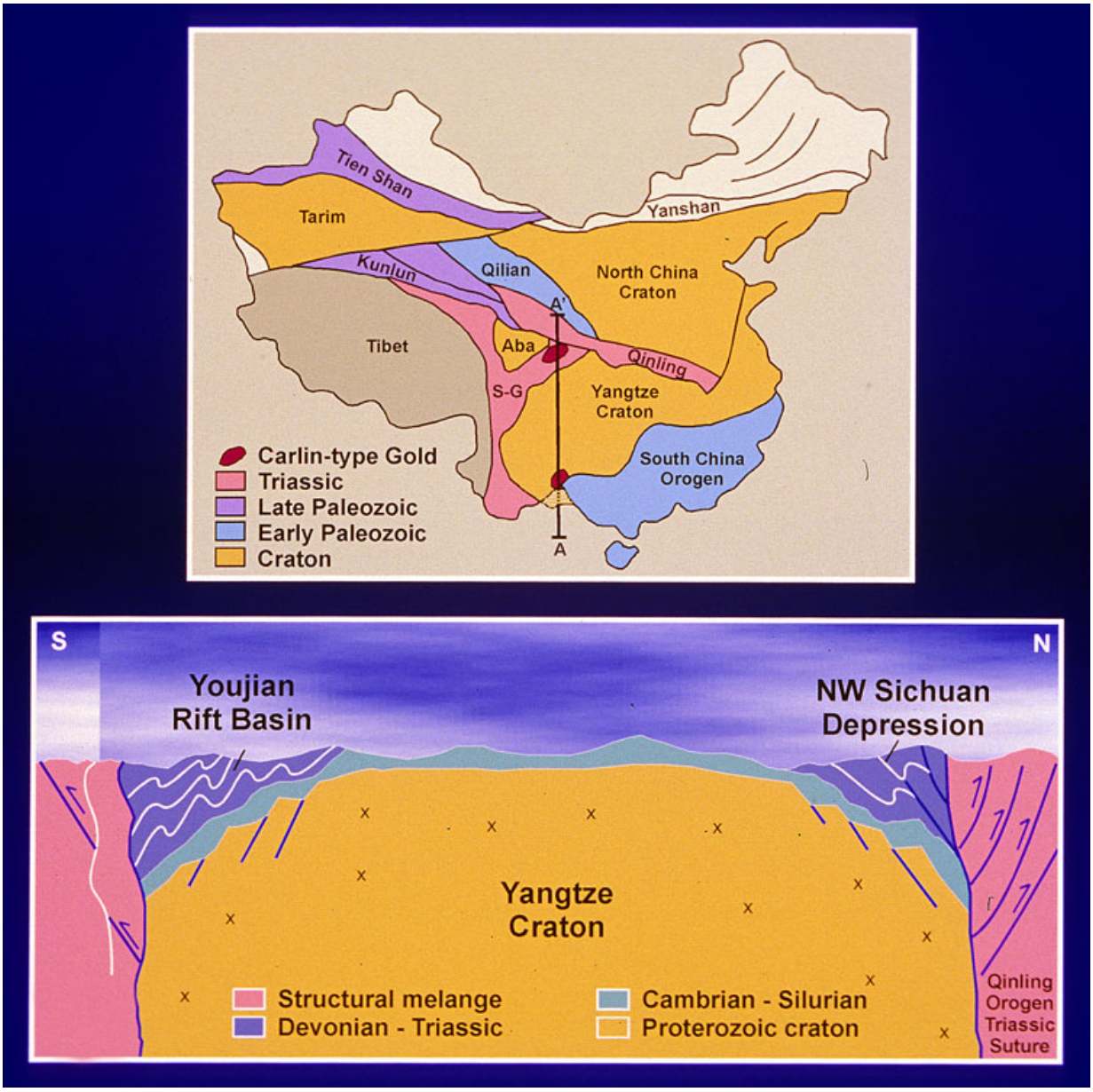

Figure 2-24. Tectonic setting of Carlin-type Au deposits in China. (*A*-top) Deposits, occur in two areas on the south and north sides of the Yangtze craton. (*B*-bottom) Cross-section through Yangtze craton (see text).

The tectonic setting in China has some similarities to that in Nevada. The map on figure 2-24 shows that Carlin-type Au deposits are present in two areas on the south and north sides of the Yangtze craton. In late Proterozoic to Silurian time, the craton was mantled by a thin sequence of siliciclastic and platform carbonate rocks. In the Devonian, the southwest and northwest margins of the craton underwent extensional faulting and deposition of a thick sequence of Devonian to Triassic carbonate and siliciclastic rocks. In the Early Triassic, the Yangtze craton collided with North China along the Qinling orogenic belt. This was followed, in the Late Triassic, by accretion of the Indochina block along a southwest-dipping subduction zone. The cross-section on figure 2-24 shows how the miogeoclines were affected by these events. Contractional deformation in both areas continued into the Jurassic. In the Qinling belt, post collisional magmatism of Triassic and Jurassic age affected the entire orogen whereas in the southern area subduction-related magmatism was restricted to the Indochina block (shown in pink on the left side of the cross section).

Figure 2-25 shows that the bulk of the Au in both areas in China is hosted in Triassic sedimentary rocks, but that host rocks also extend downward into Devonian and Cambrian sedimentary formations. In each area, if the deposits formed during a single metallogenic event, therefore they must be younger than their Triassic host rocks. Given that they are localized by faults in folded rocks, they are generally thought to be Jurassic or younger in age.

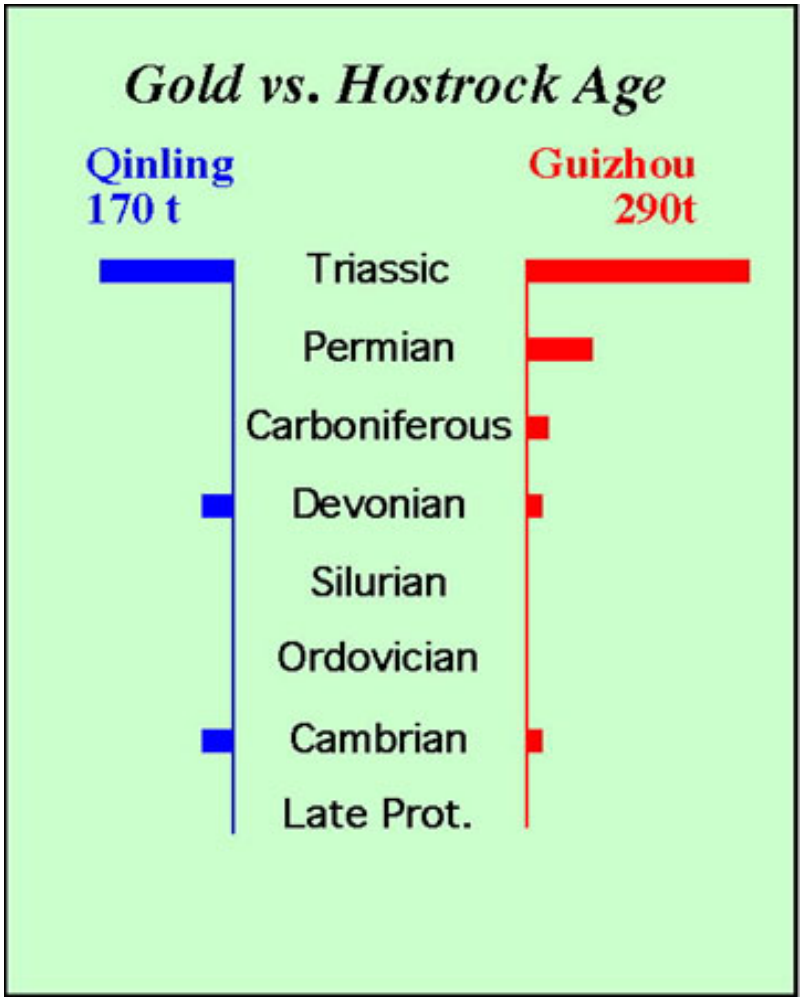

Figure 2-25. Graph showing that the bulk of Au in both areas in China is in Triassic sedimentary rocks and extends down into Devonian and Cambrian formations. The deposits are therefore younger than their Triassic host rocks.

GOUIZHOU AREA

The Guizhou area contains many geologic features that are similar to other areas. On the map (fig. 2-26), Devonian through Permian (Emeishan) rocks are in dark gray, Late Permian basalt flows are in black, and Triassic rocks are in green. You can see that the folds are fairly broad and open except in a few places. Most of the deposits are associated with faulted anticlines. Aeromagnetic surveys of this area suggest that a mosaic of basement blocks underlies the sedimentary rocks. Further evidence of deep faults is provided by the eruption of mantle-derived basalts during Late Permian extension. There also is stratigraphic evidence of syn-sedimentary faulting throughout the basin and, by some accounts, Devonian sedex deposits are present in the Dachang district on the east side of the map. It is therefore possible that some of the rocks in this area were enriched in Au by sedex processes. The Carlin-type Au deposits in the Guizhou area are thought to be Cretaceous in age because one deposit is younger than diabase dikes dated at 140 Ma. You can see that there is no evidence for a magmatic arc, leading us to wonder where the thermal energy came from to drive the hydrothermal systems. Otherwise, the geology of these deposits is very similar to those in Nevada. Figure 2-27 shows that Au ore deposits (in red) are localized by unconformities, shale/limestone contacts, folds, and faults.

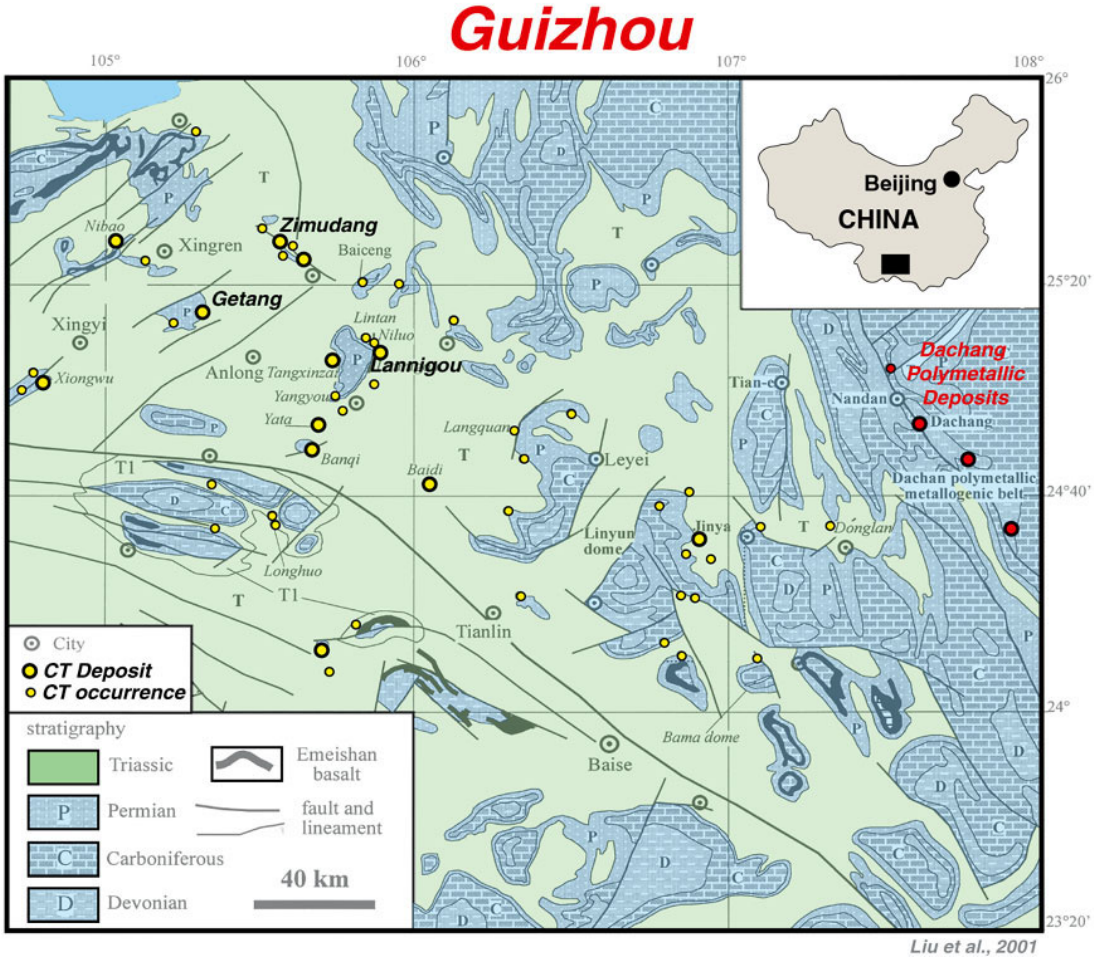

Figure 2-26. Geology and sedimentary rock-hosted Au deposits in the Guizhou (Dian-Qian-Gui) area. Most deposits are spatially associated with domal structure and lie near the interface between late Paleozoic and Triassic rocks.

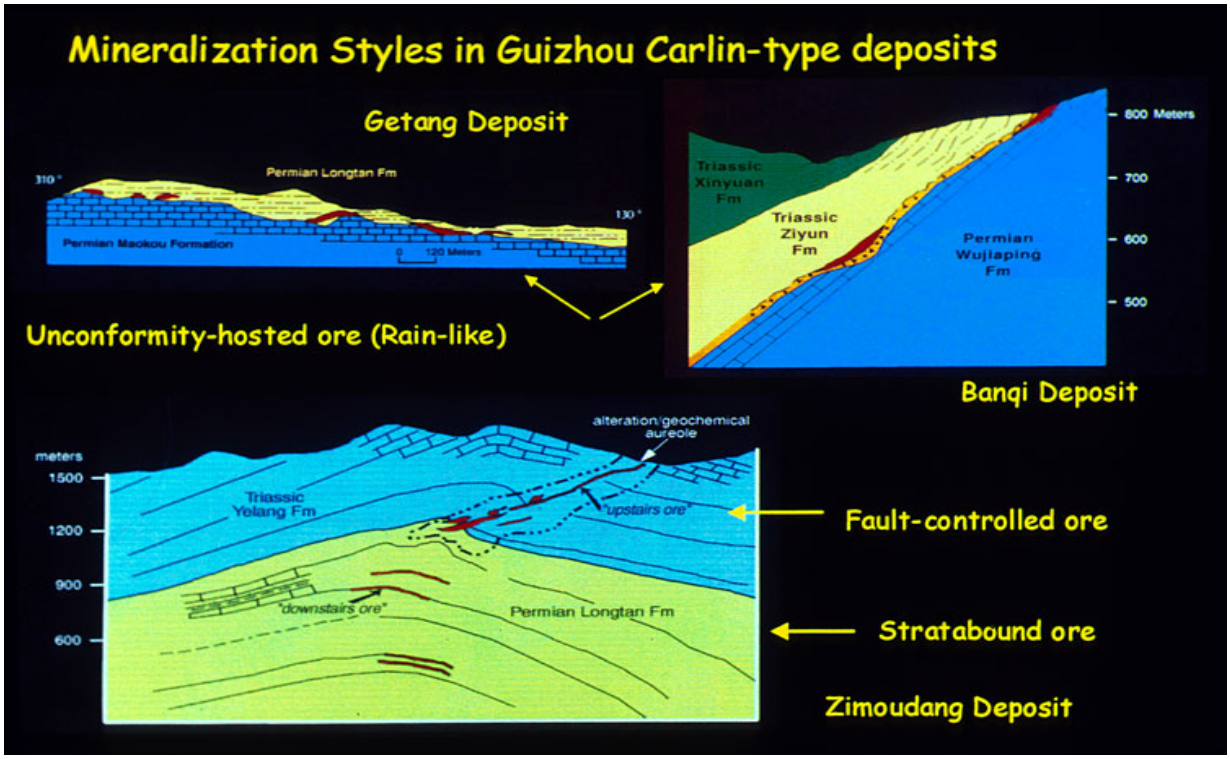

Figure 2-27. Mineralization styles in the Guizhou area for Carlin-type deposits. The unconformity-hosted (Getang), structure-hosted (Banqi), and fault-controlled (Zimudang) deposits represent the different mineralization styles.

QINLING AREA

The geologic setting of the Qinling belt, China is quite different than the Guizhou area. The generalized geologic map (fig. 2-28) is near the Liba deposits on figure 28. It shows that Au is mined from orogenic, skarn, Carlin-type, and placer Au deposits. The schematic cross section through the Qinling orogenic (fold) belt (fig. 2-29) shows that the orogenic Au deposits are located in highly deformed greenschist grade metamorphic rocks between the Shangdan and Mianlue (Lixian-Shanyong fault on fig. 2-28) suture zones. Carlin-type deposits are located in the foreland fold and thrust belt south of the Mianlue suture in weakly metamorphosed rocks.

Orogenicand Carlin-type Au deposits in this belt appear to have formed at about the same time, following peak deformation, metamorphism, and magmatism. So, it is possible that the Carlin-type deposits are a shallow expression of the orogenic deposits. Two of the Carlin-type deposits in this area are younger than Jurassic dacite dikes. It is therefore possible that they are pluton-related or that they formed by circulation of meteoric fluids during uplift and extension. A good example of Carlin-type deposits is the large Dongbeizhai Au deposit.

The Dongbeizhai Au deposit is the largest Carlin-type Au deposit in the Qinling area containing more than 50 tonnes Au and it is the only deposit that we have isotopic data for. Rocks in this area are folded and weakly metamorphosed, but there are no intrusions. Gold orebodies (in red on fig. 2-30) form lenses that are confined to the Kuashiya shear zone with little dissemination outward into the unbrecciated rocks.

Figure 2-28. Generalized geologic features of the West Qinling area, China.

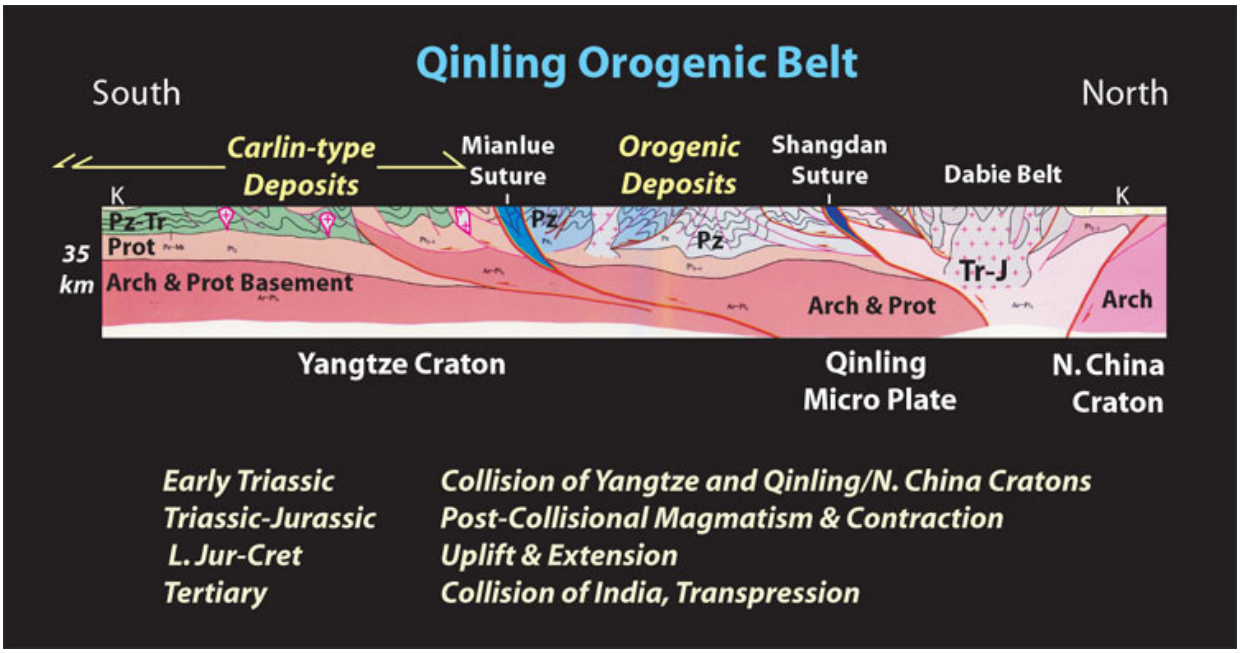

Figure 2-29. Schematic cross section through the Qinling orogenic belt, looking west.

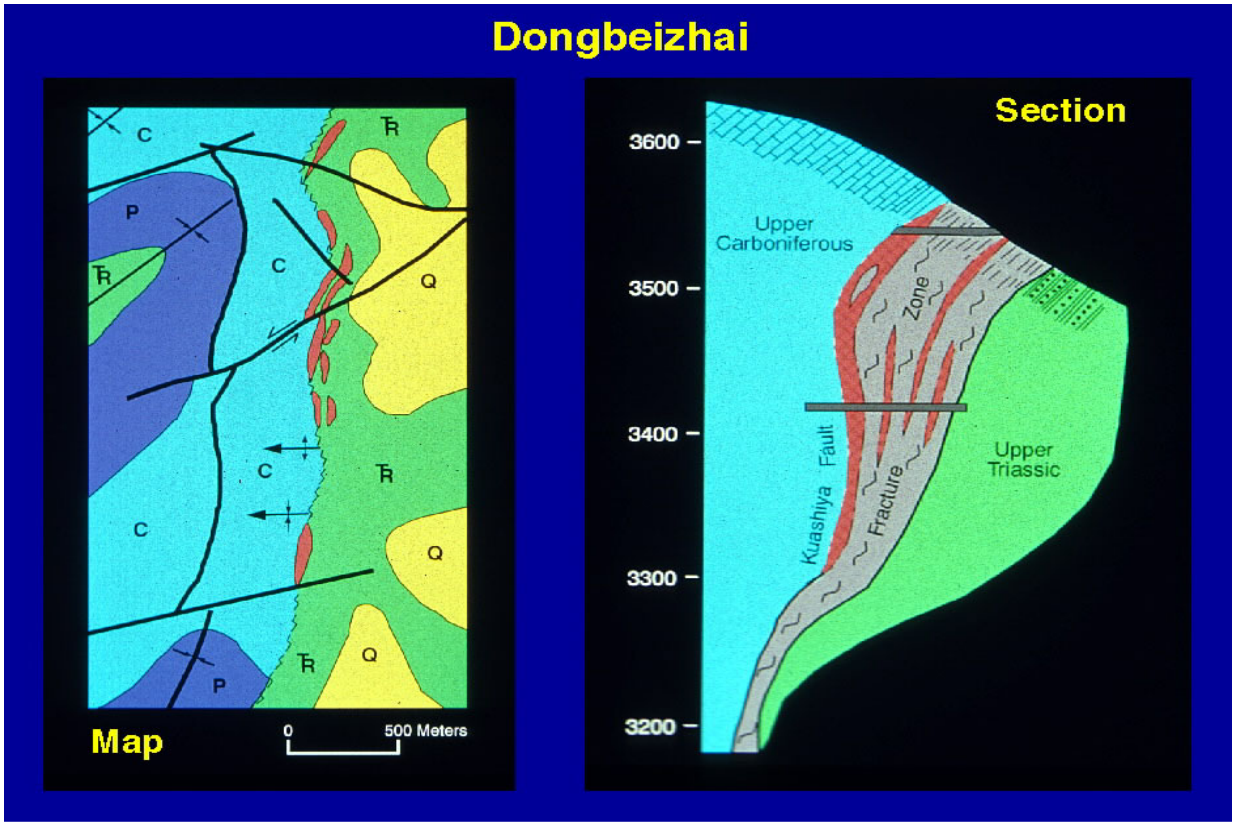

Figure 2-30. Geology and cross section of the Dongbeizhai Au deposit, Qinling area, China.

MESEL Au DEPOSIT

In Indonesia, the Mesel Au deposit is located on the north arm of Sulawesi in a classic island-arc setting (fig. 2-31 inset) that also contains porphyry Cu and volcanic-hosted epithermal deposits. It is hosted within a Middle Miocene sedimentary section composed of limestone, calcareous mudstone, and mixed lithologies of carbonate and volcanic sedimentary rocks (fig. 2-32). The carbonate section was deposited on, and later covered by, andesitic volcanic rocks (fig. 2-31). The environment of deposition was probably very similar to the numerous small, structurally controlled carbonate reef-and-lagoon environments that currently rim the arc. A porphyritic andesite body, which is in part sill-like, intruded the carbonate rocks. Gold ore is localized along high-angle faults in altered carbonate rocks below and adjacent to the intrusion. Sulawesi evolved in the complex convergence zone between the Eurasian, Philippine Sea, and Australian plates. Currently active volcanoes in the Mesel area represent the southern end of the Sangihe arc, a northwest-dipping subduction zone. Subduction related magmatism appears to have been continuous along this section of the arc for the past 15 m.y. over the entire time period in which the carbonate rocks were deposited, intruded, mineralized, covered by volcanoclastic, and exposed by erosion.

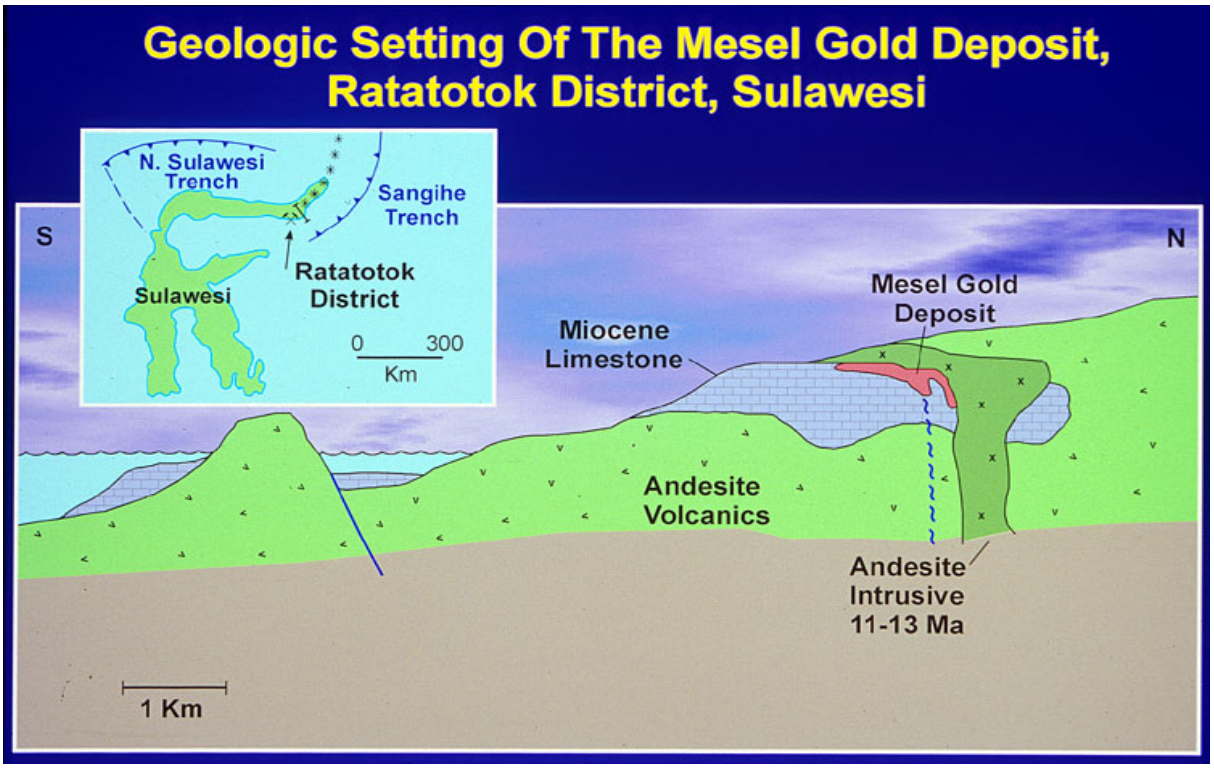

Figure 2-31. Geologic setting of the Mesel Au deposit, Ratatotok District, Sulawesi, Indonesia.

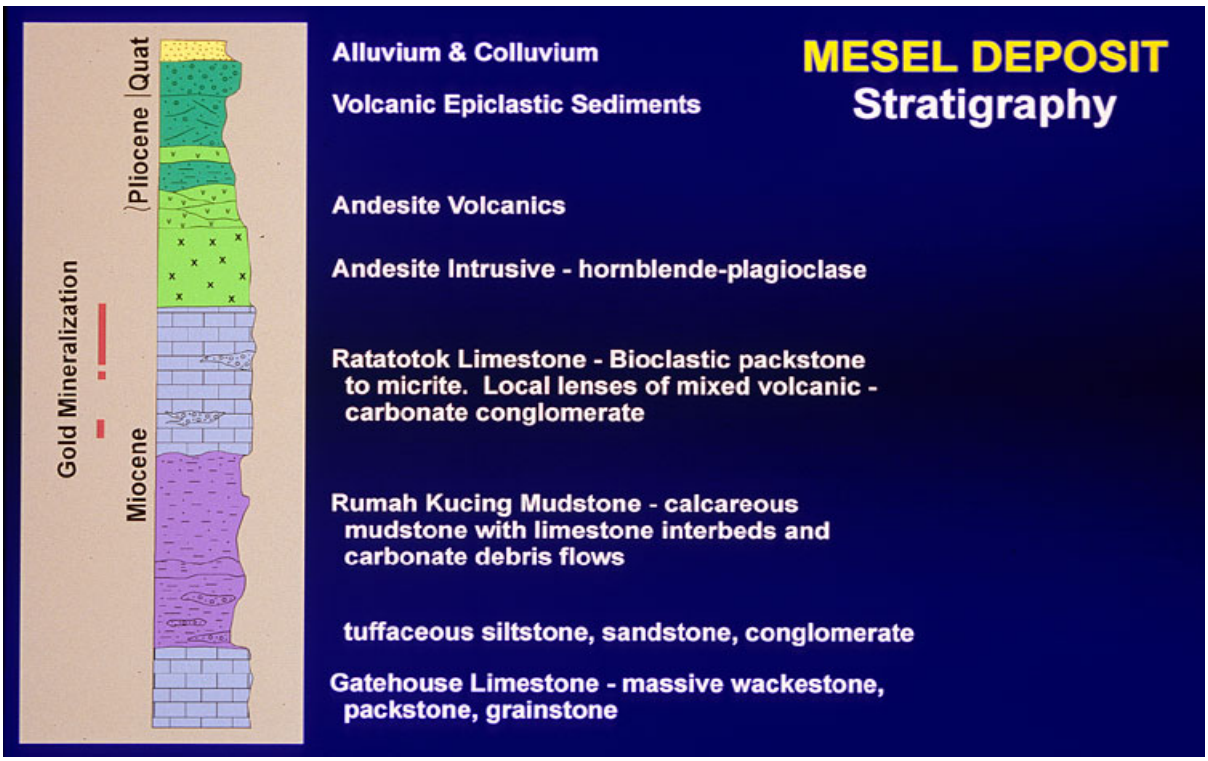

Figure 2-32. Stratigraphic section at the Mesel Au deposit, Indonesia, showing location of Au ore in the Ratatotok limestone.

SOURCE of WATER, CO_2, and H_2S

Stable isotopes assist in determining the source of water, CO_2, and H_2S in ore fluids. Most of the Carlin-type Au deposits in Nevada plot in the hachured area on figure 2-33. They have low hydrogen values and a wide range of oxygen values that extend well away from the meteoric water line. The low hydrogen values are a reflection of the cool climatic conditions that existed in the Mid-Tertiary. The wide range of oxygen values suggest that ore fluids consisted of variably exchanged meteoric water. Data from the Getchell trend covers the entire triangular range of values on figure 2-33. The samples with the highest H values are early in the paragenesis. This indicates that Au was introduced by a deep-sourced fluid that was metamorphic or magmatic in origin. The triangular range of values suggests that this fluid mixed with variably exchanged meteoric water. Deep-sourced fluids have not been detected in the other districts in Nevada.

Data from Carlin-type Au deposits in the Guizhou and Qinling areas (red and blue on fig. 2-34) are consistant with models involving the circulation of Late Jurassic or Cretaceous meteoric water when the climate was warm. In the Guizhou area, the lack of igneous or metamorphic rocks make it unlikely that deep sourced fluids were present. At Dongbeizhai, the rocks are weakly metamorphosed and not so far away from plutons and orogenic Au deposits, making it possible that deep sourced fluids were involved.

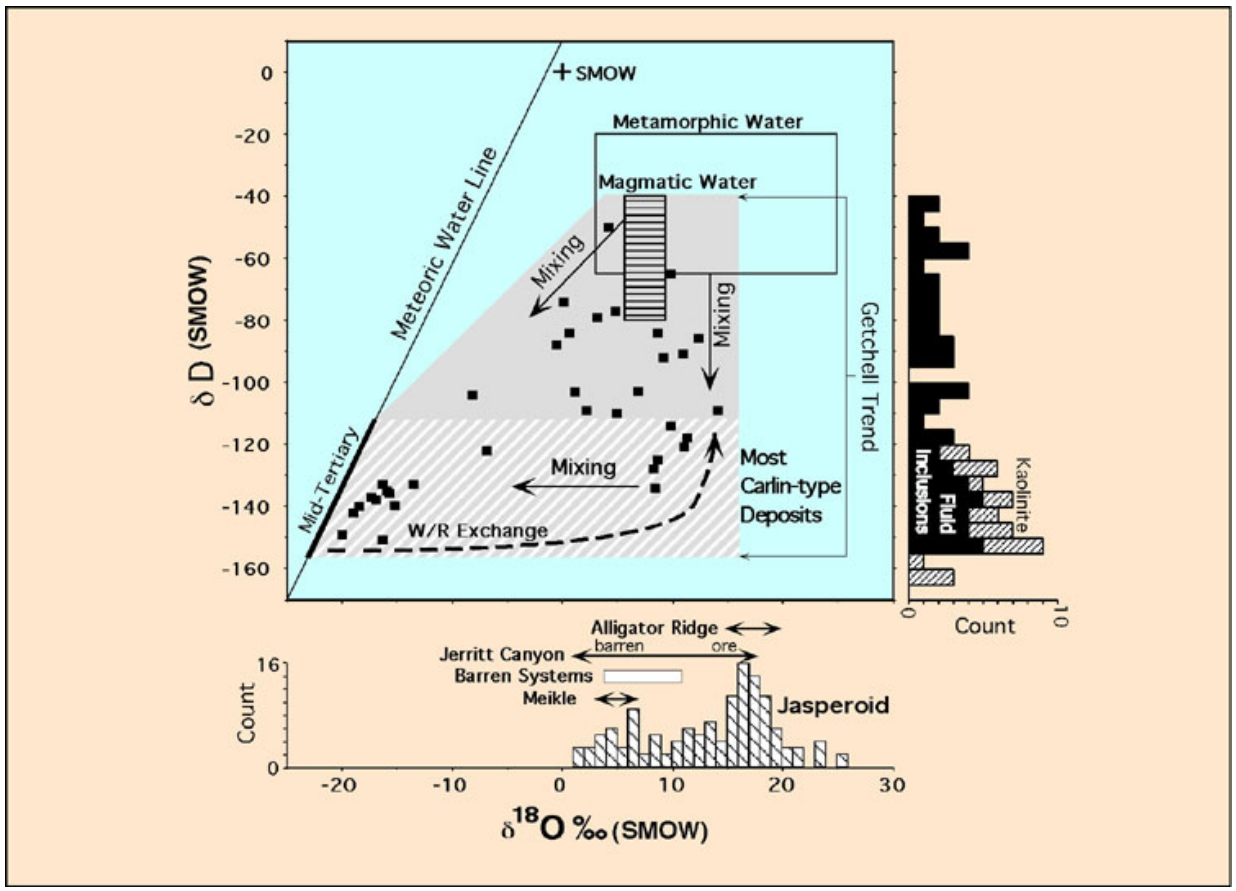

Figure 2-33. δD vs. $\delta^{18}O$ plot from Carlin-type Au deposits in northern Nevada.

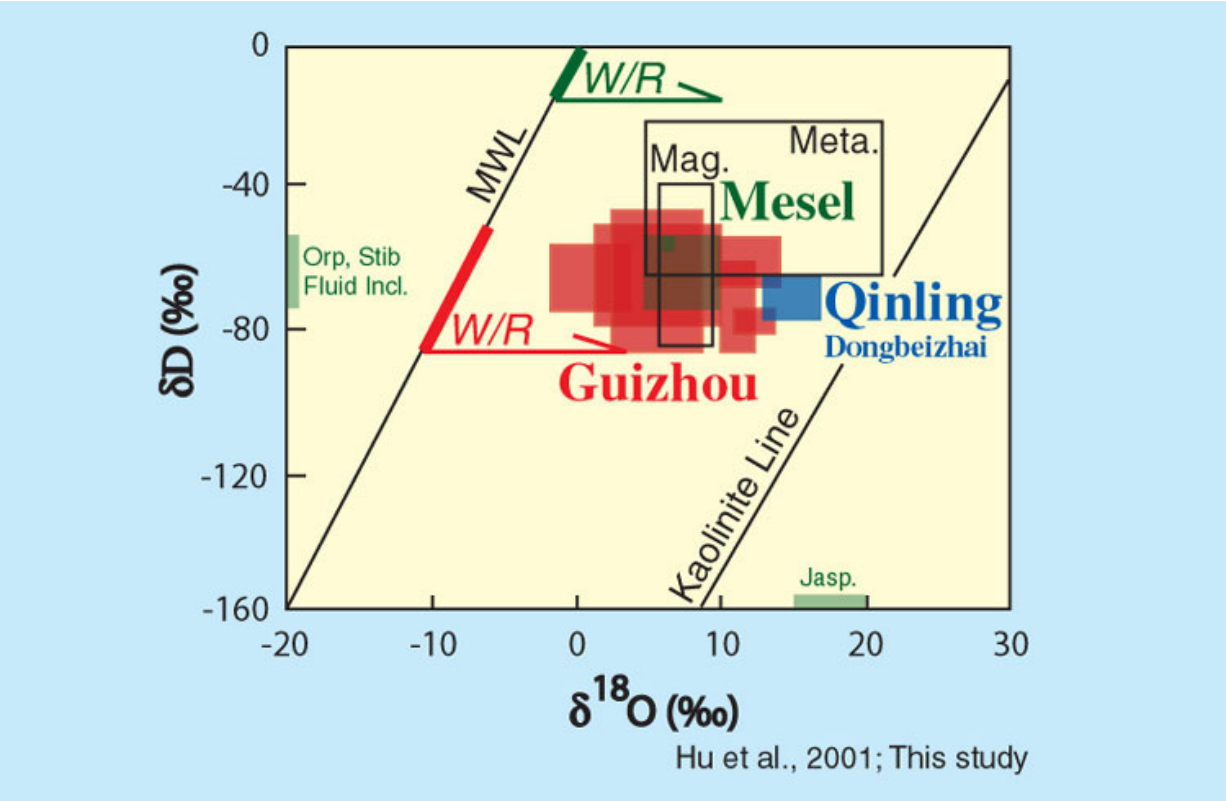

Figure 2-34. Stable isotopic data from deposits in the Guizhou and Qinling areas (red and blue).

Data from the Mesel Au deposit (green on fig. 2-34) plot in the magmatic water box with little or no contamination by warm equatorial meteoric water.

The source of CO_2 in Nevada Carlin-type (fig. 2-35) is estimated from carbon and oxygen data obtained from altered rocks that define arrays, which extend towards the isotopic composition of late calcite veins. Data arrays from deposits in the Carlin trend, Jerritt Canyon, Cortez, and Alligator Ridge districts, all converge on a similar range of values. The oxygen values are consistent with exchanged meteoric water. The high carbon values suggest that CO_2 was derived mainly from the dissolution of limestones ± partial reduction of CO_2 to CH_4 by organic matter in the host rocks. In contrast, late calcite veins from the Getchell trend (orange trapezoid; fig. 2-35) define a distinctly different array with a negative slope that is consistant with a deep magmatic or metamorphic source of CO_2.

Late calcite veins from deposits in China define several divergent arrays with negative slopes (bottom panel on fig. 2-36). Given the lack of igneous intrusions in the Guizhou area, this is best explained by dissolution of carbonate by exchanged meteoric waters with variable amounts of CO_2 derived from oxidation of organic matter. The data from Dongbeizhai Au deposit (blue arrow on bottom panel, fig. 2-36) are similar, but do not exclude a deep fluid component. At Mesel (top panel on fig. 2-36), late calcite veins formed from un exchanged meteoric water. Dolomite in mineralized andesite and CO_2 extracted from fluid inclusions in orpiment indicate that CO_2 was derived from dissolution of limestones by magmatic fluids. Although there must have been some magmatic CO_2 in the system, it was negligible in comparison to that generated by the dissolution of limestones.

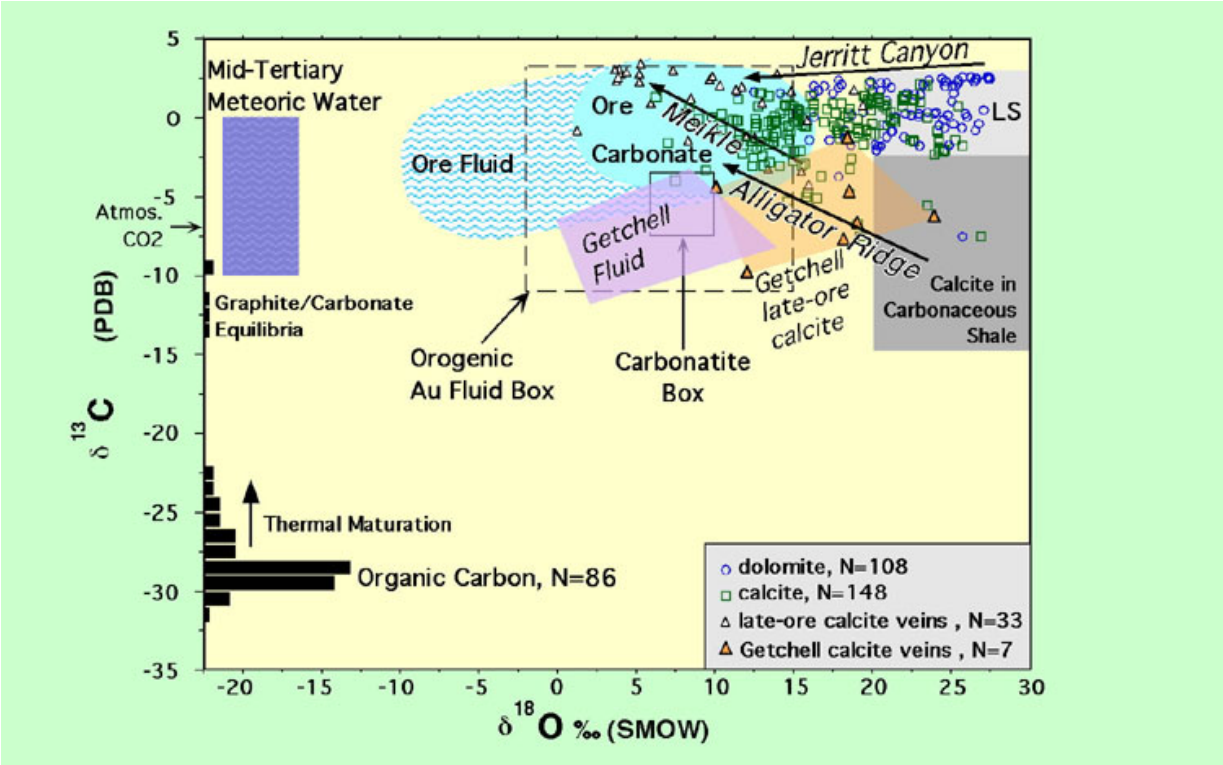

Figure 2-35. Plots of $\delta^{13}C$ vs. $\delta^{18}O$ data from altered rocks of late calcite veins from deposits in the Carlin trend, Jerritt Canyon, Cortez, and Alligator Ridge districts, northern Nevada.

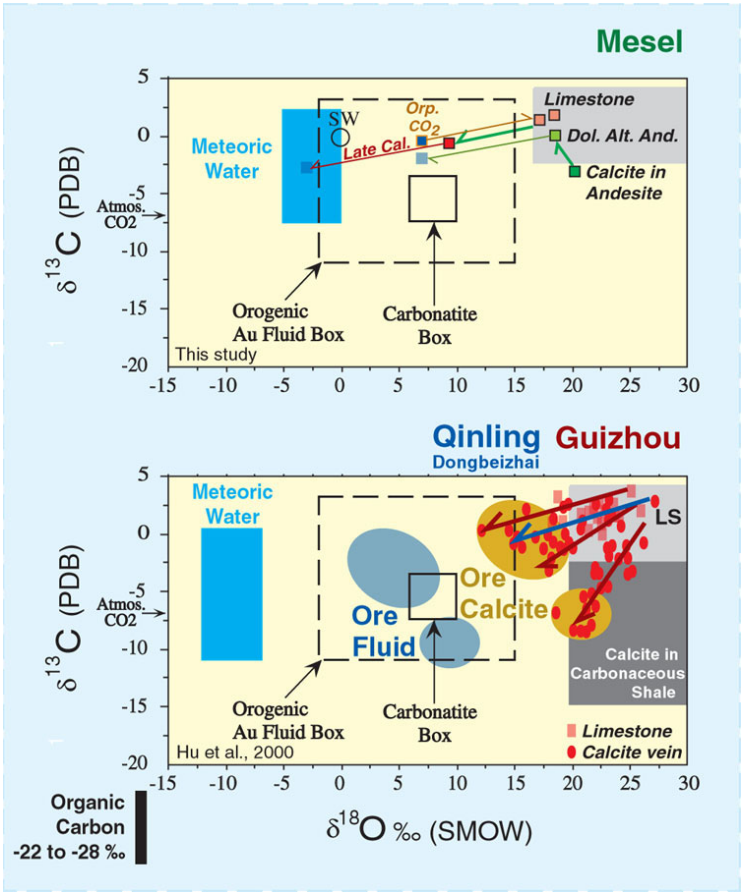

Figure 2-36. $\delta^{13}C$ vs $\delta^{18}O$ plots of data from the Mesel Au deposit, Indonesia (top panel) and Qinling and Guizhou areas, China (bottom panel).

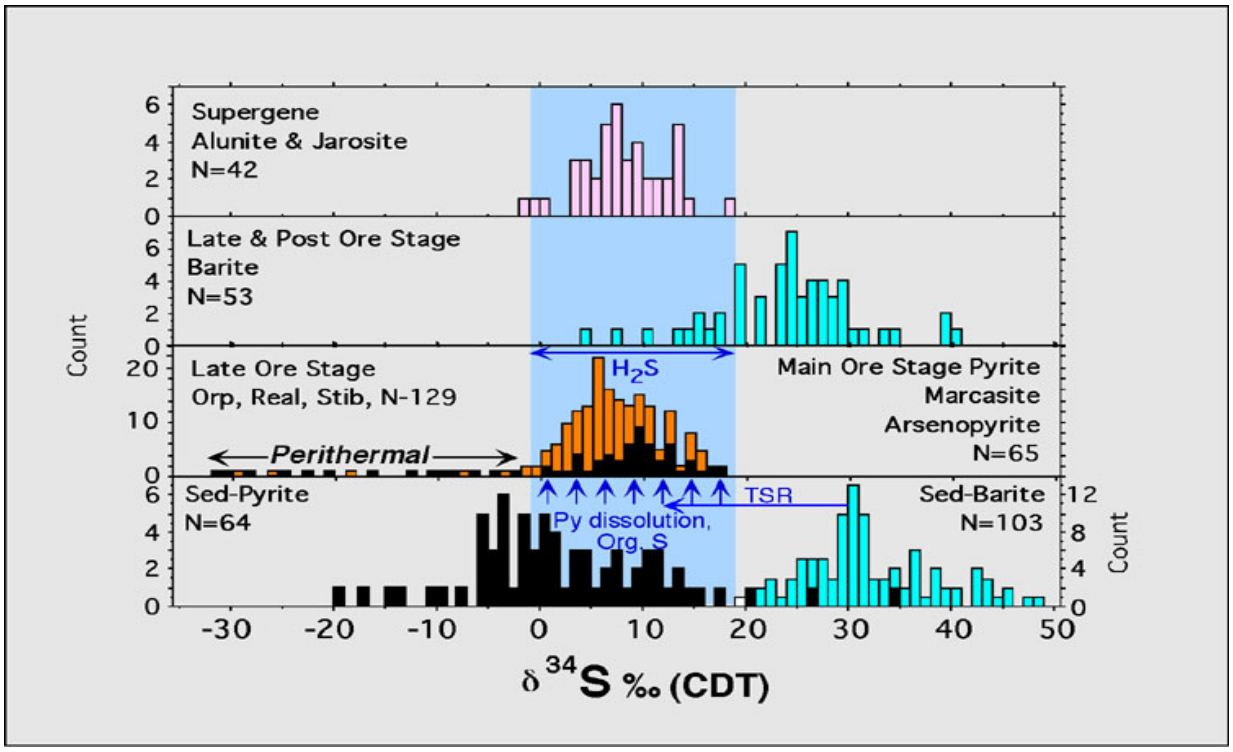

Figure 2-37. Plots of $\delta^{34}S$ data from sedimentary rock-hosted and Carlin-type Au deposits in northern Nevada.

The source of H_2S is reflected in sulfur isotopic data from deposits in Nevada as shown in figure 2-37, where the lower panel shows data for pyrite and barite in Cambrian to Mississippian host rocks. The next panel (fig. 2-37) shows data for ore stage iron sulfides (in black) and late orpiment, realgar, and stibnite (in orange). The calculated range of values for H_2S in ore fluids is shown by the blue field. The plot clearly shows that the isotopic composition of H_2S overlaps that of diagenetic pyrite. The blue vertical arrows show that some of the H_2S could have been generated by dissolution of pyrite, or at deeper levels, by metamorphic desulfidation of pyrite. The H_2S may also have been derived from the leaching or breakdown of organic sulfur compounds. The blue horizontal arrow shows that the highest sulfur values require that some H_2S came from incomplete thermochemical or inorganic reduction of sedimentary barite. The entire range of values is consistent with derivation of H_2S from sedimentary sources. If plutons were involved, they mainly provided the heat necessary to drive circulation of local ground waters. Data from Getchell extends from 0 to 8 ‰ consistent with metasedimentary or magmatic inputs of H_2S.

The sulfur isotopic data from Carlin-type Au deposits in China show similarities to similar data in Nevada (gray panel on fig. 2-38). Marine sulfate is shown in white, diagenetic pyrite in black, ore pyrite in yellow, realgar in red, and stibnite in blue. In the Guizhou deposits, ore pyrite, realgar, and stibnite have sulfur values that are very similar to the diagenetic pyrite in the host rocks. This suggests that H_2S was locally derived. Since Au was transported as a bisulfide complex, then it too may be locally derived. If so, the host rocks deserve further study to determine whether or not they were enriched in Au prior to ore formation. Sulfur data from Dongbeizhai also suggest that H_2S was derived from sedimentary or metasedimentary sources.

Sulfur data from the Mesel Au deposits is at the top of the diagram on figure 2-38. Late orpiment, realgar and stibnite have a narrow range of values near 0‰ that is consistant with a magmatic source of H_2S. Data from the carbonate-hosted ores span a wide range from –2 to—32 â, which may reflect the relative proportions of diagenetic and ore pyrite in the samples.

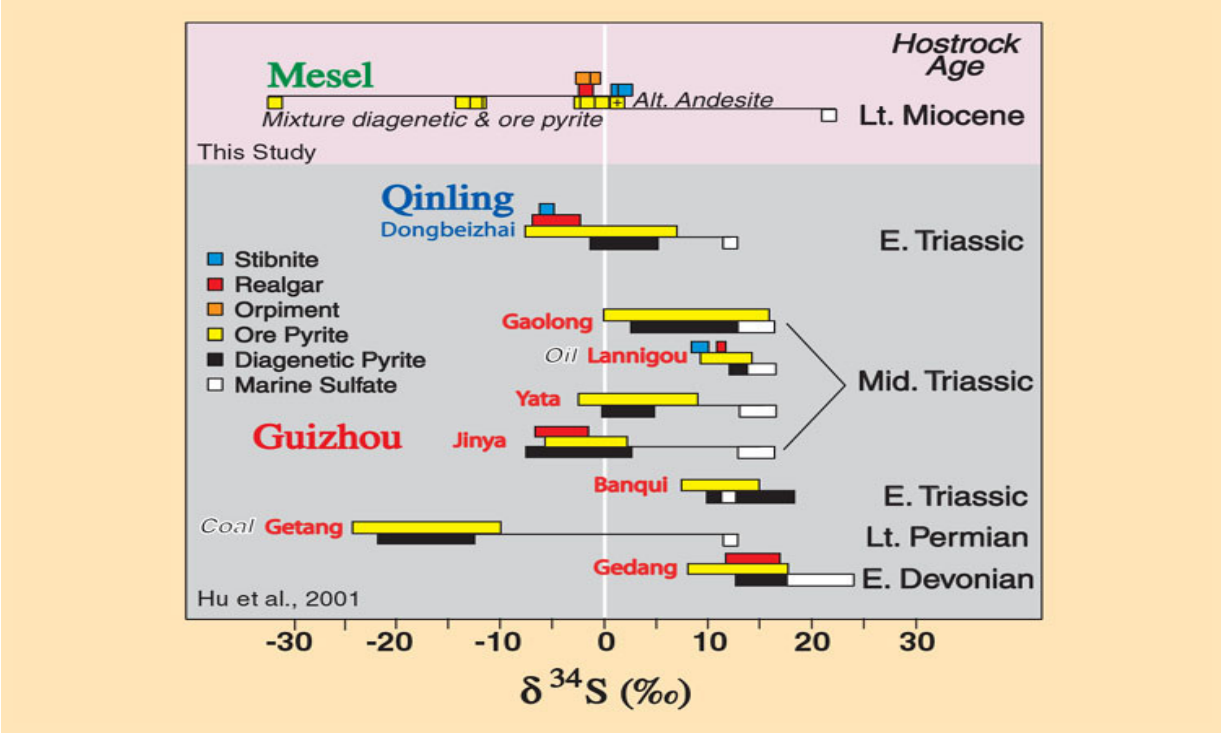

Figure 2-38. Plots of $\delta^{34}S$ data from sedimentary rock-hosted and Carlin-type Au deposits in Qinling and Guizhou areas in China and the Mesel Au deposit in Indonesia.

SUMMARY and CONCLUSIONS

What have we learned? Although the deposits in each of these areas are strikingly similar, we find that they occur in different tectonic settings and formed from different fluids (fig. 2-39). Nevada, Qinling, and Mesel areas are in magmatic arcs where there was plenty of thermal energy to drive the systems. In Guizhou, the source of heat is unclear. Perhaps the heat was provided by concealed sills associated with the Cretaceous diabase dikes. We really don't know. In Nevada, if we rely on the best isotopic data available, we need two models; a deep fluid model for the Getchell trend, and a meteoric-circulation model for the other districts. If deep fluids are present in the other districts, they are masked by an overwhelming amount of meteoric water. In China, although deep fluids are permissive in the Qinling belt, the deposits in both areas likely formed by circulation of meteoric water during uplift and extension of their respective orogenic belts. In contrast, the island-arc setting and isotopic data from Mesel Au deposit clearly show that it is pluton-related.

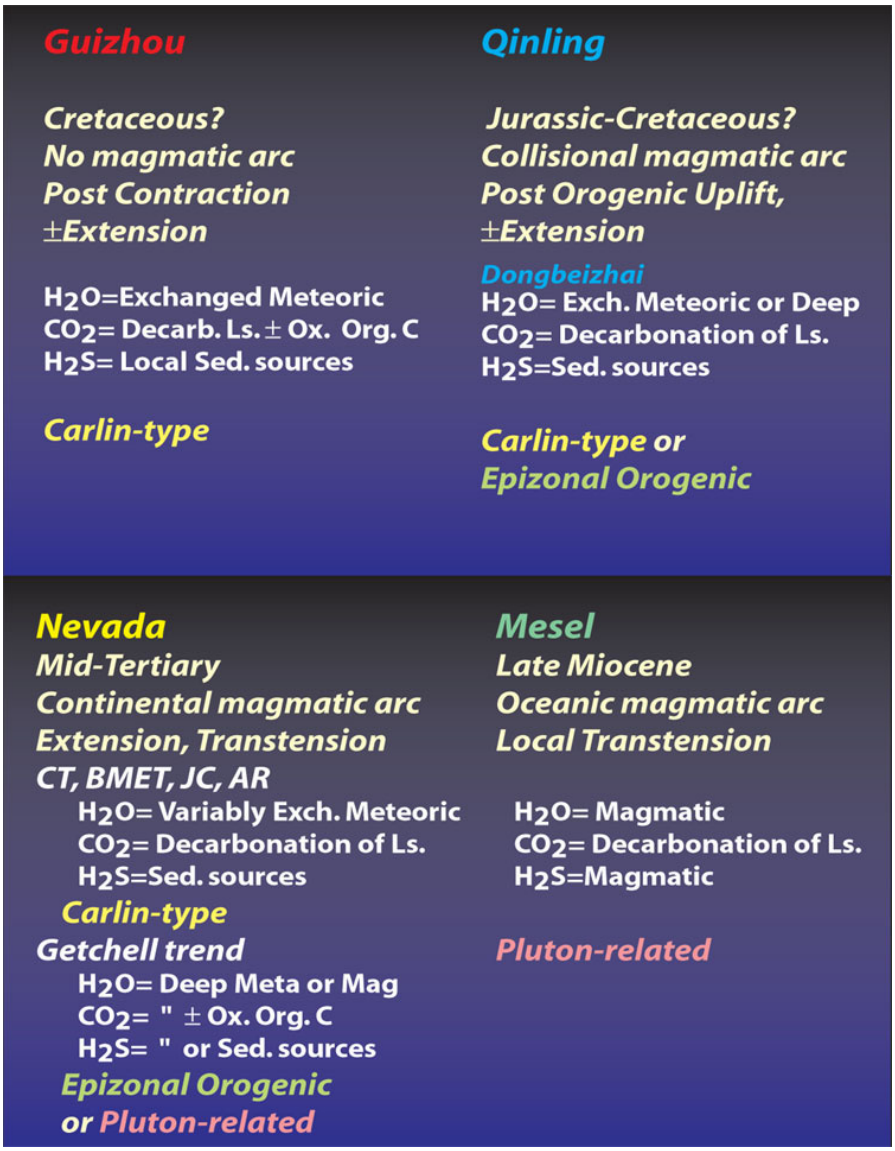

Figure 2-39. Summary of characteristics and features of Carlin-type Au deposits in China, Mesel Au deposit, Indoneaisa and Nevada.

This exercise has shown that the Carlin-type Au deposits in these districts do not neatly fit into any one genetic model. It appears that in different settings H_2S-rich fluids of diverse origins can produce very similar deposits (e.g. fig. 2-40). From an exploration standpoint, it is therefore important not to exclude areas from potential for Carlin-type Au deposits because their settings differ from that in Nevada.

These differences also raise the issue of what to call these deposits. Should we simply use Carlin-type as a catchall term or devise a new classification scheme that splits them into genetic subtypes? In our view, it is valuable to know which type you are dealing with in a particular area because they have different exploration models and different endowments of Au. Therefore, an important research frontier is simply to improve understanding of the tectonic setting, age, and types of deposits present in each area.

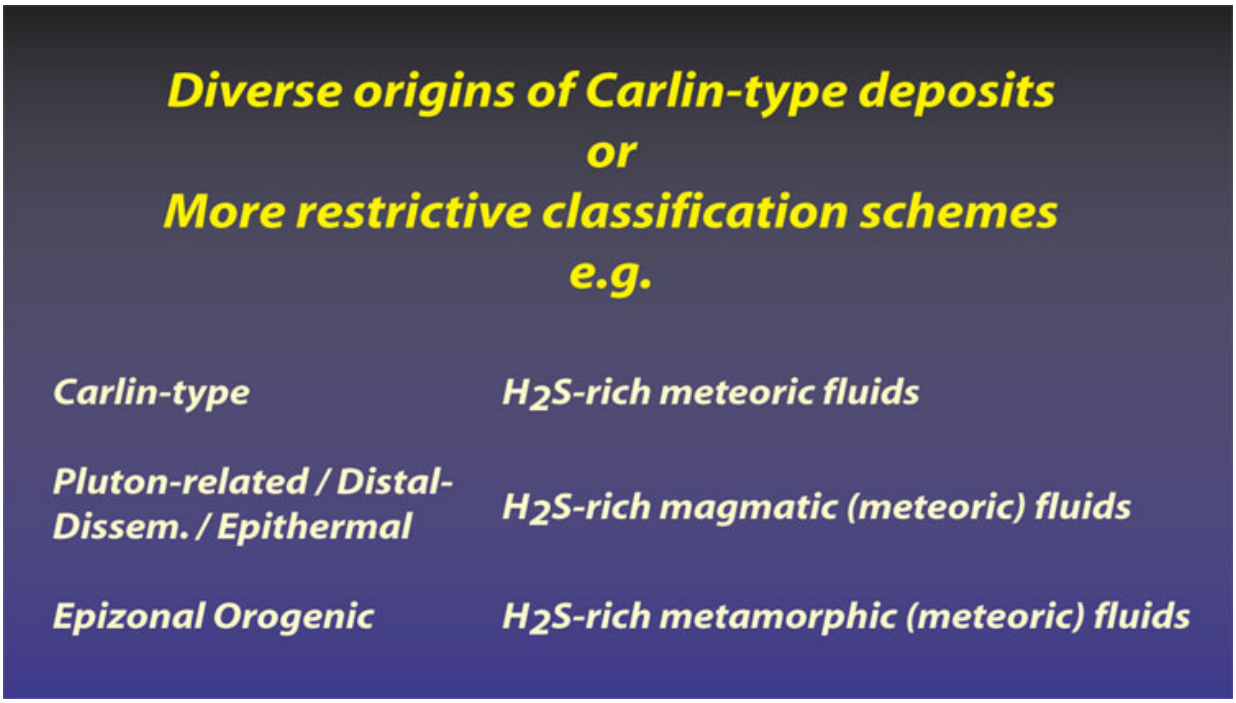

Figure 2-40. Diverse origins of Carlin-type deposits in terms of fluid sources.

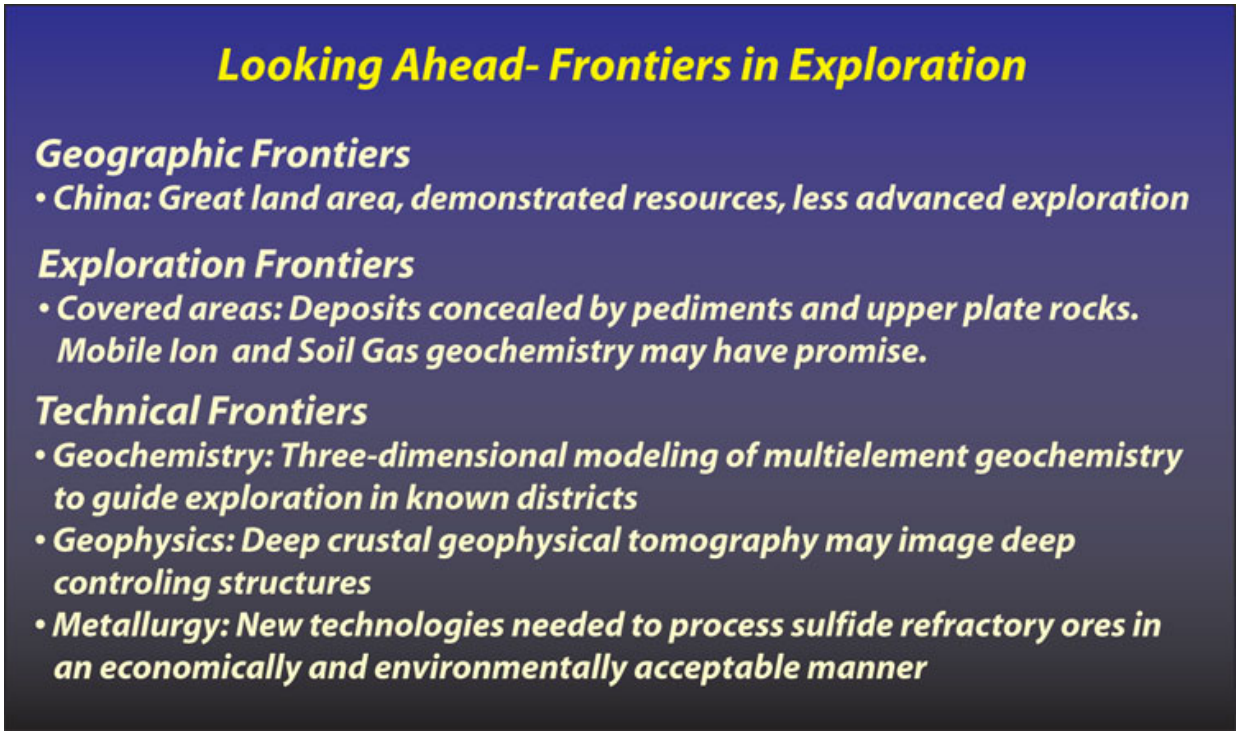

Figure 2-41. Frontiers in Exploration for Carlin-type Au deposits.

Figure 2-41 lists some frontiers in exploration for Carlin-type Au deposits. Where will the next Carlin-type districts be found? From a geologic perspective, the best bet is China. With its great land area, numerous deposits and occurrences, and less advanced exploration, it is promising terrane. In well-explored areas like Nevada, the best places to search for new deposits are beneath the cover of pediments and upper plate rocks. There is some evidence, that mobile ion or soil gas chemistry may prove their value in these areas. For continuing exploration in known districts, some companies are beginning to focus upon the three-dimensional distribution of elements other than Au. The distribution of every element tells a different part of the geologic story, and together with a sound understanding of the deposit and district geology, is critical for effective exploration. Where are the deep feeders? New seismic imaging arrays may better locate these structures or identify new ones to be explored. Metallurgical challenges remain. In Nevada, more Au remains discovered, but more is undeveloped in sulfide refractory ores than has been produced to date. Advances in metallurgical processing will be necessary to profitably extract the Au from these ores.

REFERENCES

Garwin, S.L., Hendri, D., and Lauricella, P.F., 1995, The geology of the Mesel sediment-hosted gold deposit, North Sulawesi, Indonesia, in Mauk, J.L. and St. George, J.D., eds., Proceedings of the 1995 PACRIM Congress The Australasian Institute of Mining and Metallurgy, Publication Series No 9/95, p. 221–226.

Hofstra, A.H. and Cline, J.S., 2000, Characteristics and models for Carlin-type gold deposits, Chapter 5, in Hagemann, S. G. and Brown, P.E., eds., Gold in 2000, Reviews in Economic Geology, v. 13, p. 163–220.

Hofstra, A. H. and Christensen, O.D., 2000, Carlin-type gold deposits: Defining characteristics, district comparisons, genetic models, and exploration frontiers: Society of Economic Geologists Janus II Symposium-Mineral Exploration for the 21st Century, Geological Society of America Annual Meeting, Reno, NV, Abstracts with Programs, v. 32, no. 7, p. A3.

Hu, R.Z., Su, W.C., Bi, X.W., Tu, G.Z., and Hofstra, A.H., 2001 (in press), Geology and Geochemistry of Carlin-type Gold Deposits in China: Mineralium Deposita, 26 pages, 4 tables, 10 figures. DOI-10.1007/s00126-001-0242-7.

Li, Z.P. and Peters, S.G., 1998, Comparative geology and geochemistry of sedimentary rock-hosted (Carlin-type) gold deposits in the People's Republic of China and in Nevada, USA: U.S. Geological Survey Open-File Report 98–466 (version 1.3 on CD-ROM or World Wide Web at URL http://geopubs.wr.usgs.gov/open-file/of98-466/).

Liu, J., Zheng, M., Liu, J., and Su, W., 2000, Geochemistry of the La'erma and Qiongmo Au-Se deposits in the western Qinling Mountains, China: Ore Geology Reviews, v. 17, p. 91–111.

Liu, J., Ye, J., Ying, H., Liu, J., Zheng, M., and Gu, X., 2001 (in press), Sediment-hosted micro-disseminated gold deposits in Youjiang basin, South China: Part 1, Geological and Fabric Features: Mineralium Deposita.

Mao, J., Yumin, Q., Goldfarb, R., Zhang, Zaochong, Garwin, S., and Ren, F., 2001 (in press), Geology, distribution, and classification of gold deposits in the western Qinling belt, central China: Mineralium Deposita. DOI 10.1007/s00126-001-0249-0.

Turner, S.J., Flindell, P.A., Hendri, D., Harjan, I., Lauricella, P.F., Lindsay, R.P., Marpaung, B., and White, G.P., 1994, Sediment-hosted gold mineralization in the Ratatotok district, North Sulawesi, Indonesia: Journal of Geochemical Exploration. 50, p. 317–336.